

**FUNDAMENTAL STUDIES OF CLAY SURFACE TREATMENTS TO  
FACILITATE EXFOLIATION**

Presented to the Graduate Council  
of Texas State University-San Marcos  
in Partial Fulfillment  
of the Requirements

for the Degree

Master of SCIENCE

by

Elizabeth Ann Peterson, B.S.

San Marcos, Texas  
May 2005

## ACKNOWLEDGEMENTS

I would foremost like to thank Dr. Gary Beall for all of his support during my undergraduate and graduate years. With his guidance and unbounded knowledge of polymer and physical chemistry world I have succeeded in accomplishing one of my goals. I also appreciate Dr. Chad Booth and Dr. Debra Feakes for sitting on my committee and revising my thesis.

I would furthermore like to thank my family for with out their vast help I would not have been able to do this. Thank you for everything, Dad, Mom, Billy, Brian, and Wilbur.

## TABLE OF CONTENTS

|  |     |
|--|-----|
| ACKNOWLEDGEMENTS .....                         | iii |
| LIST OF TABLES .....                           | vii |
| LIST OF FIGURES.....                           | x   |
| ABSTRACT.....                                  | xii |
| 1. INTRODUCTION .....                          | 1   |
| 1.1. Background of Nanocomposites .....        | 1   |
| 1.1.1. Problems with Nanocomposites .....      | 4   |
| 1.2. Smectite Clays .....                      | 5   |
| 1.2.1. Background on Smectite Clay .....       | 5   |
| 1.2.2. Organoclay Treatments .....             | 8   |
| 1.3. Polymer-clay Nanocomposite Formation..... | 10  |
| 1.3.1. Polymer-organoclay Nanocomposites ..... | 10  |
| 1.3.2. Background of Thermoplastics .....      | 13  |
| 1.4. Analysis of Nanocomposites.....           | 15  |
| 2. EXPERIMENTAL .....                          | 17  |
| 2.1. Materials .....                           | 17  |
| 2.2. Synthetic Methods for Clays .....         | 17  |
| 2.2.1 Surface Treatment on Clay .....          | 17  |
| 2.2.2 Surface Sorption Treatment on Clay ..... | 18  |
| 2.2.3 Edge Treatment on Clay .....             | 18  |

|       |   |    |
|-------|---|----|
| 2.3   | Melt Compounding to make Nanocomposites .....                                   | 19 |
| 2.3.1 | Haake Bowl Mixer to make Nanocomposites .....                                   | 19 |
| 2.4   | Characterization Methods .....  | 20 |
| 2.4.1 | Dynamic Mechanical Thermal Analysis .....                                       | 20 |
| 2.4.2 | Tensile Testing .....   | 20 |
| 2.4.3 | X-ray Diffraction .....   | 21 |
| 3     | RESULTS AND DISSCUSION .....  | 22 |
| 3.1   | Dynamic Mechanical Thermal Analysis Results .....                               | 22 |
| 3.1.1 | Quaternary Ammonium Surface Treated Clay-polymer Nanocomposite.                 | 24 |
| 3.1.2 | Surface Sorption Polymer Treated Clay-polymer Nanocomposite .....               | 27 |
| 3.1.3 | Edge, Surface Sorption, and Surface Treated Clay-polymer<br>Nanocomposite ..... | 30 |
| 3.1.4 | Edge and Quaternary Ammonium Treated Clay-polymer<br>Nanocomposite .....        | 32 |
| 3.1.5 | Edge and Surface Sorption Treated Clay-polymer Nanocomposite .....              | 33 |
| 3.1.6 | Washed Clay-Polymer Nanocomposite .....   | 34 |
| 3.2   | Tensile Testing .....   | 36 |
| 3.2.1 | Optimized Series with all 3 Treated Clay-polymer Nanocomposite .....            | 39 |
| 3.2.2 | Edge and Quaternary Ammonium Treated Clay-polymer<br>Nanocomposite .....        | 42 |
| 3.2.3 | Edge and PPG Treated Clay-polymer Nanocomposite .....                           | 43 |
| 3.2.4 | Washed Clay-polymer Nanocomposite .....   | 45 |
| 3.3   | X-Ray Diffraction Results .....   | 46 |

|       |   |    |
|-------|---|----|
| 3.3.1 | Quaternary Ammonium Surface Treated Clay-polymer<br>Nanocomposite .....   | 48 |
| 3.3.2 | Polymer and 2HT Surface Treated Clay-polymer Nanocomposite .....  | 50 |
| 3.3.3 | Edge, PPG, and 2HT Treated Clay-polymer Nanocomposite .....   | 51 |
| 3.3.4 | Edge and 2HT Treated Clay-polymer Nanocomposite .....   | 53 |
| 3.3.5 | Washed Edge, PPG, and 2HT Treated Clay-polymer Nanocomposite ....   | 54 |
| 3.3.6 | X-ray Diffraction Pattern for 100 m.eq 2HT Nanocomposite, 100 .m.eq.<br>2HT & 4%PPG Nanocomposite, and 100m.eq. 2HT, 4% PPG, & 2% 3-<br>Aminotrimethoxy Silane Nanocomposite..... | 54 |
| 4     | CONCLUSIONS .....   | 58 |
| 4.1   | Surface Treated Clay-polyurethane Nanocomposite .....   | 58 |
| 4.2   | Surface and Sorption Surface Treated Clay-polyurethane Nanocomposite .....  | 59 |
| 4.3   | Surface, Sorption, and Edge Treated Clay-polyurethane Nanocomposite .....   | 60 |
| 4.4   | Washed, Surface, Sorption, and/or Edge Treated Clay-polyurethane<br>Nanocomposite .....   | 61 |
| 4.5   | Final Conclusion .....  | 61 |
|       | REFERENCES .....  | 63 |

## LIST OF TABLES

|  |    |
|--|----|
| Table 1: The storage modulus at 50° C for the quaternary ammonium series<br>nanocomposites .....   | 25 |
| Table 2: Storage modulus for PVP surface treatment nanocomposite .....   | 27 |
| Table 3: Storage modulus for PPG surface treatment nanocomposite .....   | 27 |
| Table 4: Storage modulus for edge treated nanocomposite at 200 and 325 mesh .....  | 30 |
| Table 5: Storage modulus for edge and surface treated clay-polymer nanocomposite ...   | 32 |
| Table 6: Storage modulus for the surface sorption and edge treated clay-polymer<br>nanocomposite .....   | 33 |
| Table 7: Storage modulus for the washed quaternary ammonium surface treated, PPG<br>treated, and edge treated clay-polymer nanocomposite ..... | 35 |
| Table 8: Tensile properties for the optimized series of the clay- polymer nanocomposite<br>.....   | 40 |
| Table 9: Tensile data for the quaternary ammonium and edge treated clay-polymer<br>nanocomposite .....   | 42 |
| Table 10: Tensile data for the clay-polymer nanocomposite without any 2HT .....  | 44 |
| Table 11: Tensile data for the washed series of nanocomposites .....   | 46 |
| Table 12: Quaternary ammonium salt 2HT nanocomposite first order x-ray diffraction<br>peak .....   | 49 |

|  |    |
|--|----|
| Table 13: PVP nanocomposite first order x-ray diffraction peak .....                                   | 51 |
| Table 14: PGP nanocomposite first order x-ray diffraction peak .....                                   | 51 |
| Table 15: Edge treatment nanocomposite first order x-ray diffraction peak .....                        | 52 |
| Table 16: Edge and 2HT treatment nanocomposite first order x-ray diffraction peak.....                 | 54 |
| Table 17: Washed edge, PPG, and 2HT treatment nanocomposite first order x-ray<br>diffraction peak..... | 54 |
| Table 18: The height ratio of the A-B plane and the Basal spacing.....                                 | 55 |

## LIST OF FIGURES

|  |    |
|--|----|
| Figure 1: Intercalated vs. exfoliated nanocomposites .....   | 1  |
| Figure 2: Gas permeability-tortuous pathway theory.....  | 4  |
| Figure 3: Crystalline structure of Montmorillonite .....   | 6  |
| Figure 4: TEM of Montmorillonite .....   | 6  |
| Figure 5: Exchange capacity for 53 and 108 milliequivalents .....  | 7  |
| Figure 6: Ethoquad and Arquad 2HT structures and a molecular model of two clay plates<br>with a quaternary ammonium in the gallery ..... | 9  |
| Figure 7: Molecular model of octadecyltrimethoxy silane on the edge of the clay<br>platelet .....  | 10 |
| Figure 8: Flow chart representing in-situ polymerization .....   | 11 |
| Figure 9: Flow chart representing the solution approach .....  | 12 |
| Figure 10: Flow chart represents melt compounding .....  | 12 |
| Figure 11: Bowl Mixer ..   | 13 |
| Figure 12: Thermoplastic polyurethane is a linear and highly crystalline molecular<br>structure .....                                    | 14 |
| Figure 13: Polyurethane elastomer .....  | 15 |
| Figure 14: The modulus is elastic response, while the energy lost is the loss modulus...   | 23 |
| Figure 15: Pristine Pellethane DMTA.....   | 24 |

|   |    |
|---|----|
| Figure 16: A graphical representation of the increasing modulus with increasing milliequivalence .....                | 26 |
| Figure 17: DMTA for the 2HT quaternary ammonium ladder series of m.eq. ....   | 26 |
| Figure 18: Graphical representation of different polymer surface treatments with respect to the storage modulus ..... | 28 |
| Figure 19: DMTA for the ladder series of PPG at 2, 4, and 6 % 325 mesh .....  | 29 |
| Figure 20: DMTA for the ladder series of PVP at 2, 4, and 6 % .....   | 29 |
| Figure 21: DMTA for the edge, PPG, and 2HT treated clay at 200 mesh.....  | 31 |
| Figure 22: DMTA for the edge, PPG, and 2HT treated clay at 325 mesh .....   | 31 |
| Figure 23: DMTA of the edge and 2HT treated nanocomposite .....   | 33 |
| Figure 24: DMTA of the edge and surface sorption (PPG) treated nanocomposite .....                                    | 34 |
| Figure 25: DMTA of washed clay nanocomposites .....   | 36 |
| Figure 26: Typical stress-strain curve for a tensile test .....   | 37 |
| Figure 27: Stress-strain curve for the pristine polymer.....  | 38 |
| Figure 28: Stress-strain curve for 100 m.eq. 2HT 4% PPG 2% 3-aminotrimethoxy silane (325 mesh) nanocomposite .....    | 40 |
| Figure 29: Stress-strain curve for 100 m.eq 2HT clay-polymer nanocomposite.....                                       | 41 |
| Figure 30: Stress-strain curve for the 100 m.eq. 2% 3-aminotrimethoxy silane nanocomposite .....                      | 43 |
| Figure 31: Stress-strain curve for 2% PPG 2% octadecyltrimethoxy silane (325 mesh) nanocomposite .....                | 45 |
| Figure 32: XRD diffraction peak derivation .....  | 47 |
| Figure 33: Bede x-ray diffraction pattern for Pellethane .....  | 48 |

|   |    |
|---|----|
| Figure 34: Bede x-ray diffraction of 95/5 Pellethane and 95 m.eq. 2HT .....   | 50 |
| Figure 35: Octadecyltrimethoxy silane (325 mesh) x-ray diffraction pattern .....  | 52 |
| Figure 36: 3-Aminotrimethoxy silane (325 mesh) x-ray diffraction pattern .....  | 53 |
| Figure 37: The x-ray diffraction pattern for the quaternary ammonium nanocomposite .                                    | 56 |
| Figure 38: The x-ray diffraction pattern for the quaternary ammonium and polymer<br>surface treated nanocomposite ..... | 56 |
| Figure 39: The x-ray diffraction pattern for the quaternary ammonium, polymer, and<br>edge treated nanocomposite .....  | 57 |

## **ABSTRACT**

### **FUNDAMENTAL STUDIES OF CLAY SURFACE TREATMENTS TO FACILITATE EXFOLIATION**

by

Elizabeth Ann Peterson, B.S.

Texas State University-San Marcos

May 2005

**SUPERVISING PROFESSOR: GARY BEALL**

The field of nanocomposites technology is growing intensively, especially in the area of polymer/clay nanocomposites [1]. Nanocomposites are a two phase system in which one phase is dispersed in the second phase on a nanometer level [2]. Current surface treatment methods have not been successful in completely exfoliating polymer/clay nanocomposites. This research developed a general method of surface and edge treatments in order to help exfoliate organoclay into a given polymer. Several general types of treatments were utilized. These included ion exchange, surface sorption of polymers, and silane edge treatment. Melt compounding of polymer and clay was conducted in a bowl mixer. Physical properties of each nanocomposite were tested by DMTA and tensile testing. X-ray diffraction was also used to determine the extent of the intercalation or exfoliation of polymer/clay nanocomposite.

## 1.0 INTRODUCTION

### 1.1 Background of Nanocomposites

The field of nanocomposites technology is growing intensively, especially in the area of polymer–clay nanocomposites [1]. Nanocomposites are a two phase system in which one phase is dispersed in the second phase on a nanometer level [2]. Polymer-clay composites range from macro scale dispersions to intercalated systems and ultimately to fully exfoliated systems. Intercalated nanocomposites have clay layers that are well stacked and ordered in a polymer matrix, while exfoliation is when clay layers have lost their long range order and are now completely dispersed in the continuous polymer matrix (figure 1) [3]. For true nanocomposite formation, the clay must be exfoliated into the system [4].

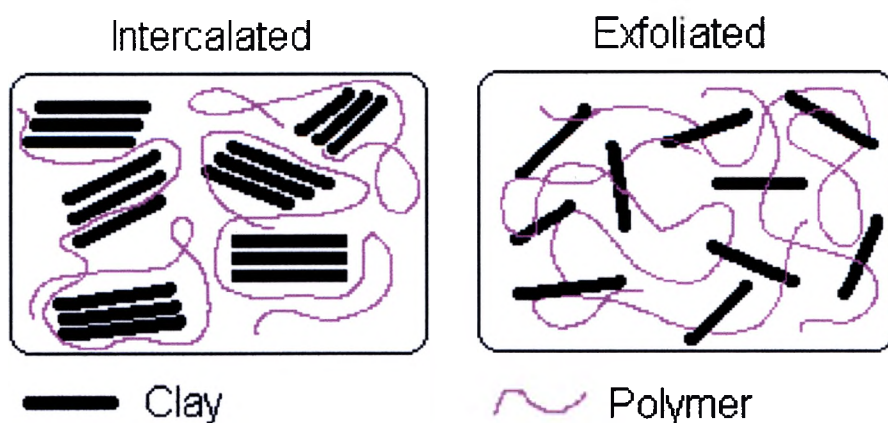


**Figure 1: Intercalated vs. Exfoliated nanocomposites**

Polymer-clay interactions have been studied since the 60's, but the first major discovery came from Toyota in the early 90's, when they discovered nanocomposite formation via in-situ polymerization [2]. This work was done using Nylon-6/clay hybrid nanocomposites made from caprolactam [6-9]. Nanocomposites containing 4 wt % of well-exfoliated ( as determined by x-ray diffraction ) silicate layers in nylon-6 showed dramatic improvements in mechanical properties, barrier properties and thermal resistance as compared to a conventional nylon 6 composites containing 20 wt % mica [6]. Specifically, the modulus doubled, the impact strength increased by 50% and the heat distortion temperature increased 80° C compared to the pristine polymer [5]. The increase in modulus and tensile strength with concurrent increase in impact had never been seen in composites before. Their improved mechanical and thermal properties extend the use of these nylon-6/clay hybrids to the automotive industry for under the hood applications [6-9].

Thermal and flammability properties are important for nanocomposites applications. The improved mechanical and thermal properties were first mentioned in 1976 by a Unitika patent application on PA-6-MMT nanocomposites [19]. The properties however were not intensely studied until J.W. Gilman and T. Kashiwagi. They quantitatively characterized the reduced flammability in a number of nanocomposites, which included exfoliated polyamide-6-MMT nanocomposites [13]. These investigations lead to the observation that flammability was reduced for both thermoplastics and thermosets without the loss of physical properties. The mechanism leading to increased flame retardation appears to be the collapse of the clay platelets during combustion which creates the multi-layer carbonaceous-silicate char layer; this appears to enhance the flame

retardation of the polymer [14]. The multi-layer carbonaceous-silicate structure acts as an insulating layer and as a physical barrier to gases which propagate the flame.

Flammability is important to widen the application of polymer nanocomposites. However, barrier properties are also a driving factor in creating new and improved nanocomposites. The food packing industry is leading the study of barrier properties with respect to clay-polymer nanocomposites. When clay is added at low loading weights to the polymer matrix the gas permeability is reduced by more than an order of magnitude. At loading weights of 1-5 wt % clay, the barrier properties show improvement without the loss of clarity in thin films [13].

The gas permeability depends on the barrier properties, which in turn relies on the aspect ratio of the dispersed particles. The aspect ratio of a characteristic clay platelet is defined as one lateral dimension divided by the thickness. As the aspect ratio for clay platelet increases, a gas permeant experiences a large increase in effective path length. The increase in the path length is not dependent on the thickness, because the permeant has to travel around the surface of the clay, which is 150-200 nm in dimension. This enlarged path length can noticeably reduce the net rate of movement across the barrier layer, thus improving the impermeability of the polymer, as shown in figure 2 [23]. The increase in path length is known as the tortuous pathway theory. This simple theory has been shown to only predict the barrier properties of a limited number of polymer nanocomposites. Another theory is that the polymer and clay have some interaction with each other which hinders the pathway of the gas molecule. This theory indicates that the movement across the nanocomposite matrix varies due to polymer-polymer interaction, polymer-clay interaction, or clay-clay interaction.

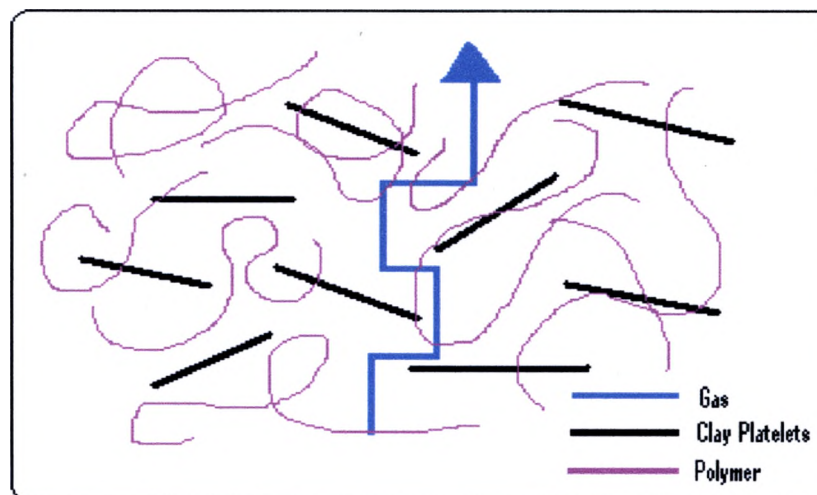


**Figure 2: Gas permeability- tortuous pathway theory.**

### **1.1.1 Problems with Nanocomposites**

Due to increased mechanical, thermal, and barrier properties, nanocomposites appear to be the material of the future. However, there are problems applying this technology to polymers other than nylon 6 and achieving full exfoliation. Nylon 6 is made from caprolactam using a chain growth ring opening polymerization. The surface modified clay is added to the caprolactam, which initiates the polymerization from the clay's surface. Nylon 6 is also made from a single monomer, while many other polymer/clay nanocomposites are made from 2 or more monomers which can lead to the clay plates being "glued" together. Another hindrance to polymer-clay nanocomposite exfoliation is the polarity of the polymer and the clay. Nylon 6 and the organoclay are polar compounds, which help to facilitate the ring opening polymerization. However, non-polar polymers and polar clays hinder the exfoliation process because non-polar polymers

do not want to enter in-between polar clay platelets. These problems will be addressed throughout this research.

## **1.2 Smectite Clays**

Smectite clays and related layered silicates are the material of choice for polymer nanocomposite design for several reasons. The first being that they exhibit a very rich intercalation chemistry, which allows them to be chemically altered and made compatible with organic polymers on the nanolevel [5]. These treatments include ion exchange, surface sorption of polymers, and edge treatment with silane coupling agents. They also occur abundantly in nature and can easily be obtained at a relatively low cost by strip mining [5]. For these reasons, smectite clays will be the focal point of this study.

### **1.2.1 Background on Smectite Clay**

Smectite clays have been successfully used in the synthesis of polymer nanocomposites, as shown by Toyota. These clays are layer silicates, such as montmorillonite, mica, laponite, and fluorohectorite [3], in which the clays have the same general structure formula and differ only in the amount and type of cation in the octahedral layer. Due to the natural abundance of montmorillonite, it will be the focus of this research.

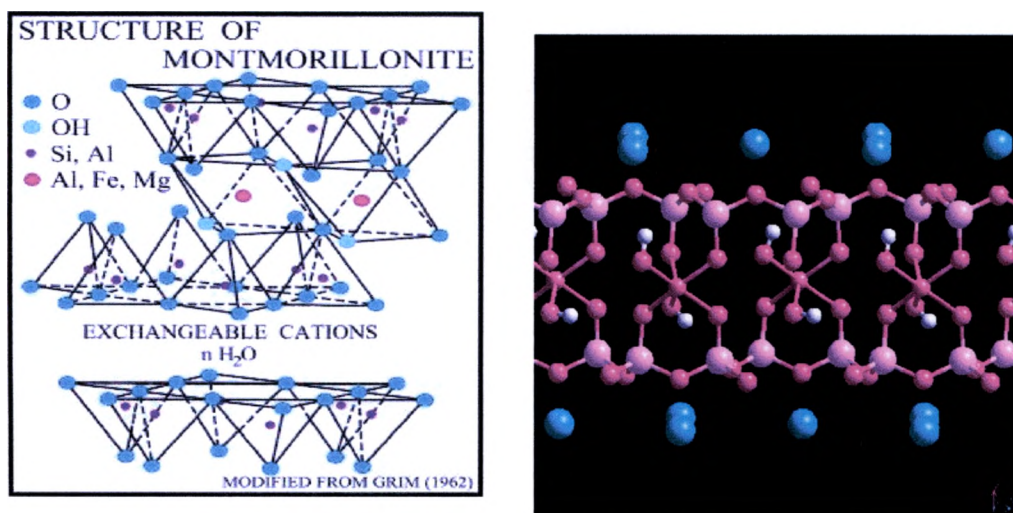


**Figure 3: Crystalline structure of Montmorillonite<sup>3</sup>**

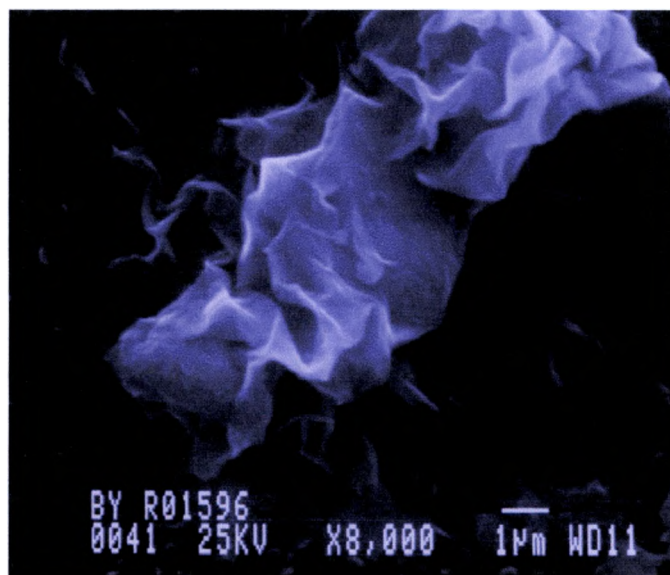


**Figure 4: Transition electron microscope picture of montmorillonite. The clay particle is actually flatter, but due to the vacuum need to take the picture it is compacted. TEM from Dr. Gary Beall.**

Montmorillonite is found all over the world due to its formation by in situ alteration of volcanic ash [1]. The volcanic ash was altered by the marine environment due to the availability of sodium and magnesium in the marine sediment. The marine environment

is the most important factor for the character of the aluminum silicate layers [1]. The crystallographic structure of montmorillonite is composed of two tetrahedral silica ( $\text{Si}_4\text{O}_{10}$ ) sheets sandwiching an octahedral sheet of either aluminum or magnesium hydroxide (figure 3). The isomorphous substitution of  $\text{Si}^{4+}$  for  $\text{Al}^{3+}$  in the tetrahedral lattice and of  $\text{Mg}^{2+}$  for  $\text{Al}^{3+}$  gives the octahedral sheet an excess negative charge that is manifested near the surface of the clay [1,3]. This negative charge is then counterbalanced by cations such as  $\text{Ca}^{2+}$  and  $\text{Na}^+$  situated between the layers of clay.  $\text{Ca}^{2+}$  and  $\text{Na}^+$  on the surface of the clay allows for the surface to be altered by exchange with organic onium ions. The amount of cations on the surface is the cation exchange capacity for the clay (figure 5). This exchange capacity is usually expressed in terms of milliequivalence per 100 grams of clay. Montmorillonite has a relatively high exchange capacity which makes it an excellent choice to use for nanocomposites. The high exchange capacity allows the onium ion treatment to render the surface hydrophobic.

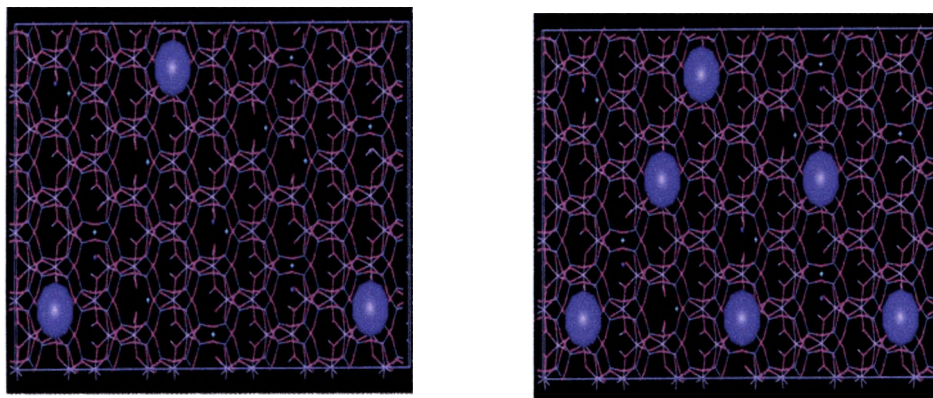


**Figure 5: The picture on the left shows 53 milliequivalent cation exchange capacity clay and the picture on the right show a 108 milliequivalent cation exchange capacity clay. Molecular modeling by Dr. Gary Beall.**

The surface of the clay which is not counter balanced by the  $\text{Na}^+$  and  $\text{Ca}^{2+}$  still maintains a small negative charge. The high polarity of the cations on the surface makes the clay extremely hydrophilic which leads to the presence of water of hydration between

the layers [3]. A problem that must be addressed is the non polar nature of most polymers and the hydrophilic nature of clay. If the surface has a charge then the polymer is not inclined to enter into the gallery (space between two clay platelets). Additionally, the edge of the clay also contributes strongly to the polarity, since they are terminated by hydroxyl groups (attached to the silicon and aluminum). This creates an activation barrier to polymer intercalation into the gallery. The edge of the clay can be modified to exchange the terminal hydroxyl groups with different functional silane groups to remove this orientation barrier.

### **1.2.2 Organoclay Treatments**

The objective of this research is to develop a general method of surface treatment, which completely exfoliates surface treated organoclays with various polymers. Several general types of treatments will be utilized including ion exchange, surface sorption of polymers, and silane edge treatment. Once the surface and edge of the organoclay have been optimized the clay will be incorporated into the polymer.

The first treatment will be the modification of the clay surface with quaternary ammonium salts, such as Ethoquad T/12 PG and Arquad 2HT-82E, produced by AKZO Nobel Surface Chemistry LLC. The quaternary ammonium salt modifies a nanoclay surface by ionically bonding to it (figure 6), converting the surface from hydrophilic to organophilic [16]. Once the most compatible quaternary ammonium salt is identified, the ammonium ion density can be varied on the silicate surface of the clay. This is accomplished by changing the milliequivalence (m.eq.) in a ladder series to cover a wide

range of concentrations. In order to judge the compatibility a given treatment imparts, thermoplastic polyurethane was chosen as a test polymer for the formation of composites.

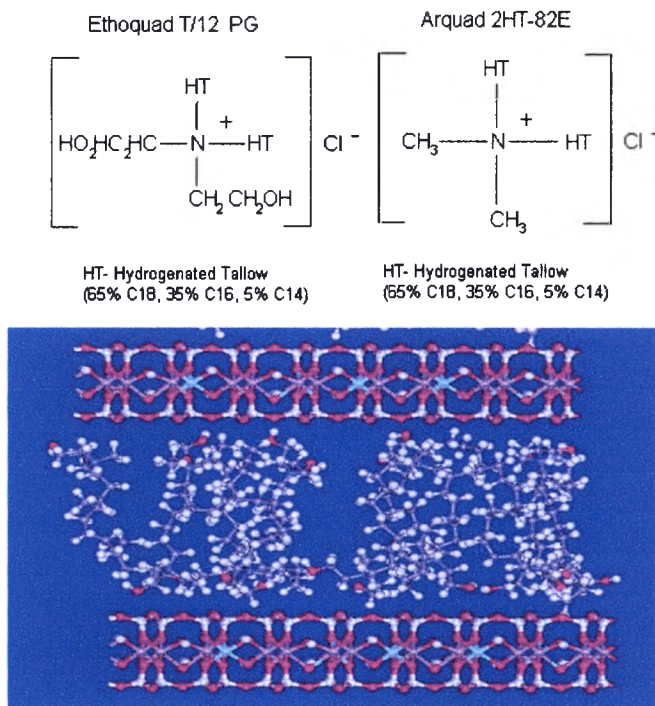


**Figure 6: Ethoquad and Arquad 2HT structures and a molecular model by Dr. Gary Beall of two clay plates with a quaternary ammonium in the gallery.**

The second treatment involves a sorption treatment on the surface of the clay platelet using polypropylene glycol (PPG) or polyvinyl pyrrolidone (PVP). This will be done in order to cover the bare surface of the silicate. Polyurethane was compounded with organoclay that was previously treated with PVP and PPG in order to find the polymer that yielded the best compatibility. DMTA was used to determine the treatment that yielded the largest change in storage modulus. The most compatible sorption treatment was then put through a ladder series of 2, 4, and 6 % wt. polyol to clay, in order to optimize the surface compatibility of the clay.

The last modification was an edge treatment. This was done to change the terminal groups from a hydroxyl group to various organic groups. Five different silanes were

examined in order to find the most compatible treatment for the edge of the clay. N-dodecyltrimethoxy silane, octadecyltrimethoxy silane, phenyltrimethoxy silane, vinyltrimethoxy silane, and 3-aminopropyltrimethoxy silane were all tested. Figure 7 shows octadecyltrimethoxy silane on the edge of the clay. One methoxy group reacts with one or more of the aluminum or silicone termination groups on the edge of the clay and releases methanol byproduct. This allows for the edge functionality of the clay.

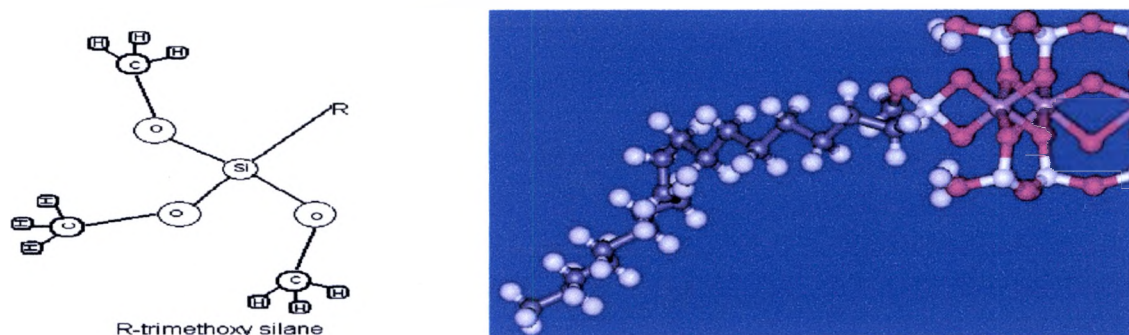


**Figure 7: R-trimethoxy silane structure and molecular model of octadecyltrimethoxy silane on the edge of the clay platelet.**

### 1.3 Polymer-clay Nanocomposite Formation

There are three major methods for nanocomposite formation: in-situ nanocomposite formation, solution nanocomposite formation, and melt compounding. Each type of nanocomposite formation has to be evaluated individually with respect to the type of polymer being processed and cost. Cost is an important factor because the main reason for studying nanocomposites is the use as engineering applications by industry. These types of applications tend to be quite cost sensitive.

#### 1.3.1 Polymer-organoclay Nanocomposites

In-situ nanocompositing was the first method demonstrated by Toyota in the development of nylon 6 clay nanocomposites. In this approach the organoclay is swollen

in the monomer and then the reaction is initiated as shown in figure 8. This type of formation is used today to make nylon 6-clay nanocomposites for under the hood applications. A draw back of this method is that it is limited to ring opening polymerization.

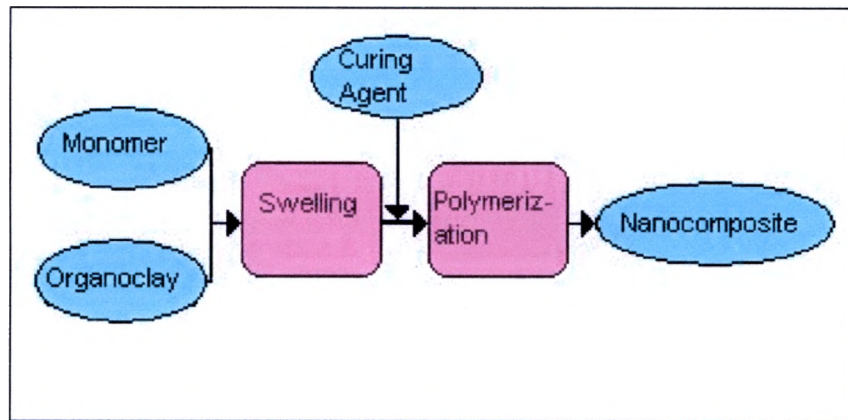


**Figure 8: Flow chart representing in-situ polymerization nanocomposite formation.**

The next type of process for producing nanocomposites is solution nanocomposite formation. The first step in solution nanocomposite synthesis is to disperse the organoclay into a solvent that allows the clay to swell and create a gel structure. The polymer is then dissolved in the solvent and intercalates between the clay layers. The last step is to evaporate the solvent, usually under vacuum and heat (figure 9). The advantage to this approach is that it allows for the possibility to form intercalated nanocomposites, with low or no polarity. A major draw back however is that it is difficult to use solution nanocomposite formation in industry since large amounts of solvent are required and the potential for volatile organic compounds (VOC) emissions is high [3].

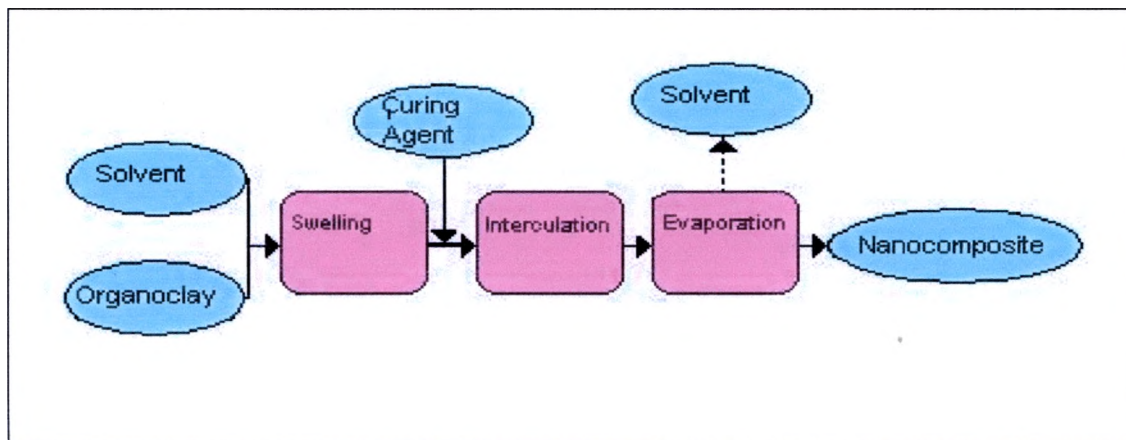


**Figure 9: Flow chart representing the solution approach.**

The last type of nanocomposite process is melt compounding, first reported by Vaia in 1993 [3]. An important aspect of melt compounding is the absence of solvent. This makes the process environmentally friendly (a green process) and cost effective. Commodity polymers such as nylon 6 and polystyrene have been melt compounded to produce conventional composites for decades. The thermoplastic polymer and the organoclay are blended in an extruder while the polymer is in its molten state [3]. The mixture is then annealed above the glass transition temperature to form the nanocomposite as show in figure 10.

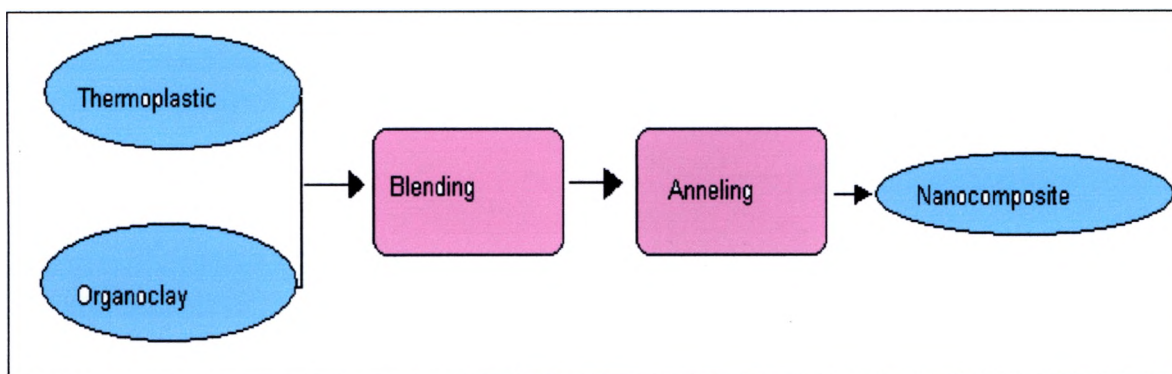


**Figure 10: Flow chart which represents melts compounding**

Melt compounding has become progressively more popular since it allows for potential application in industry by many companies that don't normally produce polymers [10]. Because of its wide popularity, melt compounding will be the main focus of this research. Each modified clay will be melt compounded into the select polymer by bowl mixing (figure 11).

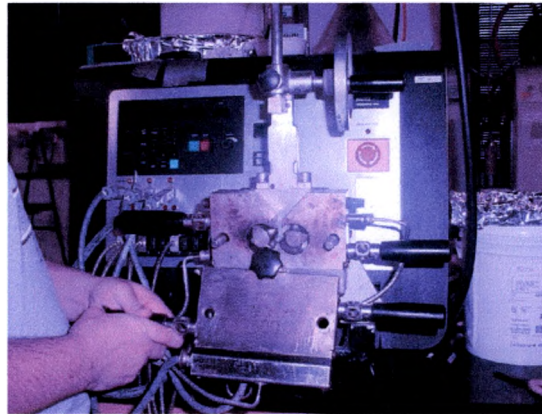


**Figure 11: Bowl Mixer**

### **1.3.2 Background of Thermoplastics**

Since melt compounding will be used as the nanocomposite formation method, a thermoplastic must be selected as the polymer. Thermoplastics are the leading choice for melt compounding for several reasons. First, thermoplastics softens when exposed to heat and return to their original condition when cooled back to room temperature [16]. Also, thermoplastics often come in pellet form and can be heated to a soft pliable material which allows for injected molding. When the material is cooled it takes the shape of the mold without a change to the initial properties of the plastic. Additionally, since no chemical curing takes place [21], the plastic can be recycled multiple times. The polymer will start to degrade after repeated heat/ cool cycles [21].

Toyota studied the thermoplastic, polyamide 6 (Nylon 6). Other thermoplastics such as poly (ethylene oxide), poly (methyl methacrylate), poly butadieneacrylonitrile, polydiacetylene, poly ( $\epsilon$ -caprolactone), polystyrene, and poly (ethylene terephthalate) have also been studied by Toyota [3]. Nanocomposites based on polypropylene are a challenge for industry since the clay does not exfoliate completely in the polymer matrix. Historically, polyurethanes (figure 12) have been classified as thermosets, but recently DuPont has produced a line of polyurethanes which are thermoplastics. Also, polyurethanes are in high demand by industry since they are used as coatings, adhesives, fibers, foams, and thermoplastic elastomers [10].

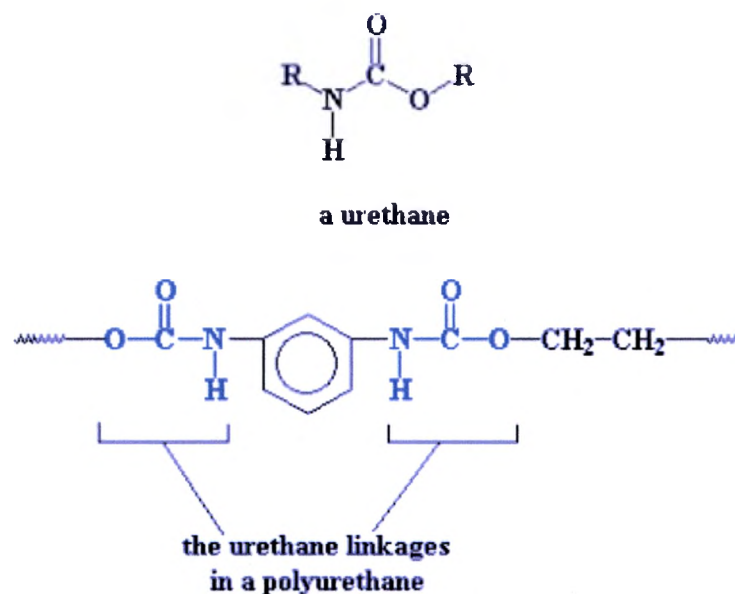
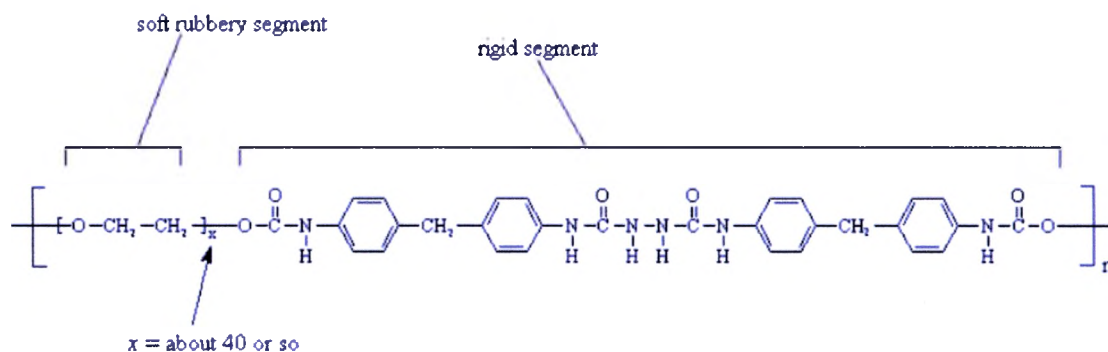


**Figure 12: Thermoplastic polyurethane is a linear and highly crystalline molecular structure [22].**

Thermoplastic polyurethanes are used throughout industry and can be elastomeric. The thermoplastic elastomer is not a true elastomer because each polymer chain does not contain at least one crosslink unit, but they are lightly crosslinked and display elastomeric properties. Thermoplastic elastomers (figure 13) contains both hard and soft segments. In

addition, most thermoplastic elastomers are non-polar and to date only polar polymers with clay have been successfully exfoliated [11]. The thermoplastic elastomer has many characteristics that are useful for this research and it was therefore chosen as the polymer for this research. These reasons include;

- it has never been successfully exfoliated
- it is fairly non-polar
- it can be melt compounded at reasonably low temperatures
- it is elastomeric and therefore will magnify the nanocomposite effect
- it has a lot of industrial applications.



Spandex has a complicated structure, with both urea and urethane linkages in the backbone chain.

**Figure 13: Polyurethane elastomer has both a soft and hard segment in the polymer chain [22].**

#### 1.4 Analysis of Nanocomposites

Once all the nanocomposites are melt compounded using the treated organoclay and the thermoplastic elastomer, the nanocomposites will be tested to examine several different properties. The first analysis will be DMTA (Dynamic Mechanical Thermal Analysis). This will be used to compare the storage modulus of each nanocomposite to that of the pristine polymer. Tensile testing will also be performed to determine the

tensile strength, Young's modulus, and the yield point of each nanocomposite. This data will be compared to that of the pristine polymer. The last analysis of the nanocomposites will be x-ray diffraction (XRD). This will be used to examine the amount of intercalation or exfoliation of each polymer-clay nanocomposite.

## **2.0 EXPERIMENTAL**

### **2.1 Materials**

A 50 lb. bag of Pellethane (which is a polyurethane elastomer) was donated by Dow Chemicals for use in this project. The sodium Cloisite clay was donated by Southern Clay Products and used for all clay treatments. The Ethoquad T/12 PG and Arquad 2HT-82E was donated by AKZO Nobel Surface Chemistry LLC. The polypropylene glycol (PPG) and polyvinyl pyrrolidone (PVP) were donated by BASF. The octadecyltrimethoxysilane of 99.8 % purity was purchased from United Chemical Technologies, Inc. and no further purification was performed. The dodecyltrimethoxysilane, 3-aminopropyltrimethoxysilane, vinyltrimethoxysilane, and phenyltrimethoxysilane were also purchased from United Chemical Technologies, Inc. and no further purification was performed.

### **2.2 Synthetic Methods for Clay**

#### **2.2.1 Surface Treatment on Clay**

The quaternary ammonium salt was placed (90, 95, 100, 105, 110 m.eq) into a clean dry 250 ml beaker and melted in a double boiler system. Once the quaternary ammonium salt melted, the Kitchen Aid was locked into position and run on low speed. The quaternary ammonium salt was added slowly to 250 g of sodium Cloisite clay, until completely combined. The beaker was then filled with 125 ml of boiling distilled water

completely combined. The beaker was then filled with 125 ml of boiling distilled water to remove any residual salt. The water was added to the Kitchen Aid containing the clay and salt mixture until the mixture had the appearance of small pea size clumps. Once the clay mixture was mixed for five minutes, it was then processed through the mini extruder (meat grinder) 2 to 3 times until steam appeared at the outlet of the extruder. The organoclay was then placed into an 80 °C oven overnight to dry. Next, it was ground with a coffee grinder and sieved at 200 mesh (75 micron grating) and 325 mesh (45 micron grating) by a sieve shaker for 1 hour. The organoclay was separated into individual plastic bags according to size to be processed later with the polyurethane elastomer (Pellethane).

### **2.2.2 Surface Sorption Treatment on Clay**

The procedure from section 2.2.1 was again followed, with the addition of the step of adding the polymer surface sorption treatment. The polymers (PVP or PPG) [2 (5 g), 4 (10 g) and 6 (15 g) % by weight of the clay (250 g)] were added to the quaternary ammonium salt while in the double boiler system. Again the procedure from 2.2.1 was followed exactly. If just the surface sorption treatment was needed, the polyol was added directly into the Na<sup>+</sup> clay without any heating or quaternary ammonium salt.

### **2.2.3 Edge Treatment on Clay**

Procedure 2.2.2 was then followed, but after the addition of the quaternary ammonium and polymer surface sorption treatment to the Na<sup>+</sup> clay, the silane [2% (5g)

by weight of clay (250 g)] was then added to the clay mixture. Following the silane addition, 125 ml of water was added as described in section 2.2.1..

If only the edge treatment and polyol treatments were needed, the polymer sorption treatment (2, 4, 6 % by weight of clay) was added into the clay first and mixed with the kitchen aid for several minutes. The edge treatment with 2% (5 g) of each silane was then added to the clay mixture. Distilled water (125 ml) was added to the mixture until the organoclay resembled small pea size clumps. It was then processed with the extruder as described in section 2.2.1 and dried over night in an oven.

If just the edge treatment was needed, the 2% (5g) of each silane was added directly into 250 g of clay and processed with 125 ml of distilled water. The organoclay was then processed through the meat grinder until steam appeared and dried overnight at 80°C to remove any excess water.

## **2.3 Melt Compounding to make Nanocomposites**

### **2.3.1 Haake Bowl Mixer to make Nanocomposites**

The organoclays described above were melt compounded to produce nanocomposites. Each nanocomposite was made at 5% by weight of the clay. The Pellethane was dried for 2 hours at 80 °C to remove any water absorbed by the polymer. Pellethane (47.5 g) and each dried clay (2.5 g) were weighed out into individual weigh boats. Then the Pellethane was added to the bowl mixer [Haake Rheomix 600 (powered by a Haake Fisons Rheodrive 5000)] at 145 °C at 30 RPM. After 5 minutes the organoclay was added. The clay and Pellethane were mixed together for 30 minutes at 145°C and 60 RPM. The nanocomposite was then cooled to 80°C and removed from the bowl mixer.

The nanocomposite was then pressed into thin films and compression molded using a Platen press and tested using X-ray diffraction, DMTA, and tensile testing.

## **2.4 Characterization Methods**

### **2.4.1 Dynamical Mechanical Thermal Analysis**

A TA Q800 series DMTA was used to perform thermal analysis. Dried nanocomposite (3g) was compression molded into a 5mm x 1mm x 20mm (width, thickness, length) mold using a Carver Model C Platen Press at 150 °C. Each bar was then secured into the thin film clamps and tested. Temperature was ranged from 30-100 °C at 5 degrees per minute.

### **2.4.2 Tensile Testing**

Each nanocomposite (28 g) was dried at 80 °C for 3 hours. Each sample was then pressed into a 50mm x 3mm x 100mm mold. Three samples were then cut out using a dog bone shaped cutter with center dimensions of 5mm in width and 3 mm in thickness. The samples remained in a desiccator until testing. Each sample was then clamped into the Sintech 1/D Tensile Tester at a gage length of 50 mm and the speed set to 15 mm per minute.

### **X-ray Diffraction**

The nanocomposites(3g) were then pressed into thin films by the Carver Model C Platen Press at 150°C for x-ray diffraction. A Bede X-ray diffractometer equipped with a Ni filter CuK $\alpha$  X-ray radiation tube was used for all of the nanocomposites tested. Each sample was placed onto the x-ray plate by using double sided sticky tape. Once the nanocomposite was secured, the x-ray was scanned from 0.5 degrees to 20 degrees 2 theta-omega.

### 3.0 RESULTS AND DISCUSSION

Each nanocomposite was made using 5% clay to 95 % Pellethane by melt compounding in a bowl mixer. Visually the nanocomposites were slightly yellow when compared to the pristine polymer, with clarity equal to that of the pristine polymer. The nanocomposites without any quaternary ammonium salt (2HT) tended to be opaque. This was attributed to the clay platelets acting as a macrocomposite in the polymer matrix, this will be discussed later. Once the visual characteristics were examined each nanocomposite was tested using DMTA, tensile test, and X-ray diffraction.

#### 3.1 Dynamic Mechanical Thermal Analysis Results

The nanocomposites were tested using Dynamic Mechanical Thermal Analysis (DMTA). This technique measures the mechanical properties of materials as a function of temperature and stress. This test was chosen as the principle measure of success, since an increase in modulus is a key characteristic of successful nanocomposite formation.

DMTA is defined by Hooke's law in which stress and strain are related through a proportional constant called the *modulus* (E or G):

Hooke's Law:  $\text{stress} = \text{modulus} * \text{strain}$

$s = Ee$  (Tension, Compression or Bending)

$t = Gg$  (Shear)

Where  $s$  and  $t$  are stress terms;  $e$  and  $g$  are strain terms. The modulus is a measure of the stiffness of a material as shown in figure 14. *Stiffness* is the ability of a material to resist deformation.

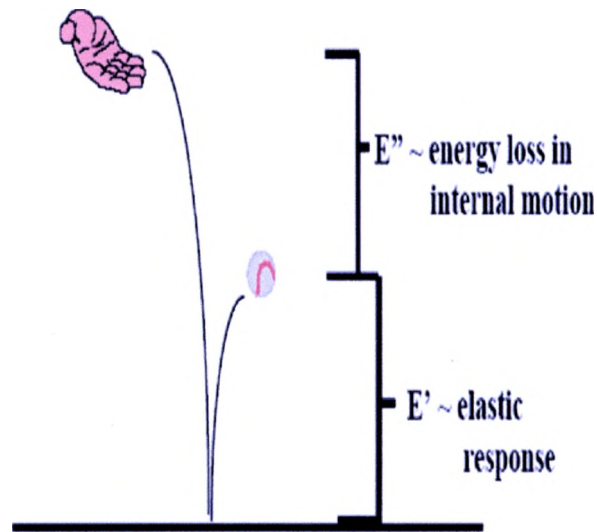


**Figure 14: The modulus is elastic response, while the energy lost is the loss modulus.**

The storage moduli taken from the DMTA data at a  $50^{\circ}\text{C}$ , are shown in the following tables. The thickness of each sample was found to be important for the testing. If the thin film was less than 1 mm thick the storage modulus would decrease by 50% or more. The change in the storage modulus is attributed to the storage modulus being so low that it was reaching the minimum detection parameters of the DMTA. Each sample was prepared by compression molding the nanocomposite into a set mold. Standardizing each sample to a set size gave a more consistent storage modulus data.

The pristine Pellethane has a storage modulus of  $15.98 \pm 2.87$  MPa at  $50^{\circ}\text{C}$  as shown in figure 15. The storage modulus for the pristine Pellethane was used to theoretically calculate the increase in modulus for a 5% wt clay-polymer nanocomposite using HALPIN-TSAI theory [24]. HALPIN-TSAI theory takes into account the aspect ratio,

loading weight, and the moduli of the polymer-clay nanocomposite to theoretically calculate the storage modulus. The theoretical storage modulus calculated varied from 16 to 60 MPa. For exfoliated clay-polymer nanocomposites the storage modulus should be at the high end of the calculation, ~ 60 MPa, while an intercalated system would have a storage modulus some where between 16 and 60 MPa. Each set of DMTA data was compared to the theoretical calculation.

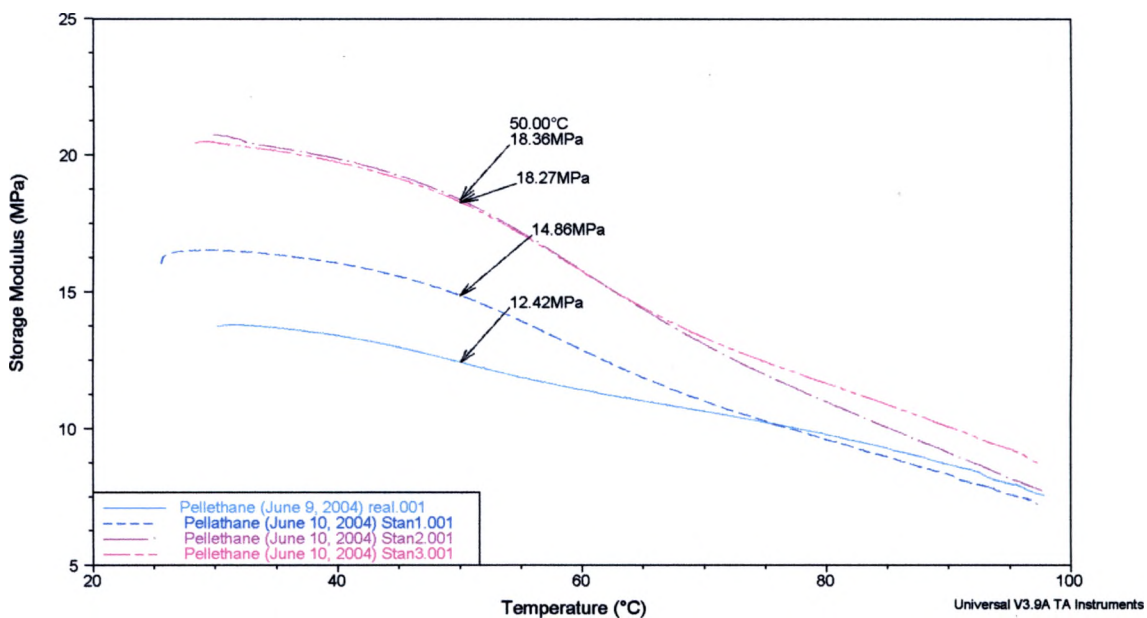


**Figure 15: Pristine Pellethane DMTA, where the mean is  $15.98 \pm 2.87$  MPa at 50 °C.**

### 3.1.1 Quaternary Ammonium Surface Treatment Clay-polymer Nanocomposite

The ladder series of quaternary ammonium salt on the surface of the clay showed improved physical properties when compared to the pristine polymer (table 1). For one system, the storage modulus for each concentration showed an approximate 100% increase at 50 °C, when compared to the pristine polymer. Also, the strength of the nanocomposites was directly related to the concentration of surface modifier, up to 105m.eq. At this point the storage modulus decreased as shown in figure 16. Figure 16

is a representation of the data collected from the graph at 50 °C. Figure 16 clearly shows that there is an optimum level of quaternary ammonium surface treatment. The curve indicates that 100 m.eq. 2HT on the surface of the clay gives the highest storage modulus at 42.50 MPa. This value is a 165% increase compared to the pristine polymer (figure 17). The experimental error for figure 17 is much better than seen in figure 15 because the DMTA is within its normal operating parameters.

Also, the clay-polymer nanocomposites with 95, 100, 105 m.eq. quaternary ammonium exchange all displayed storage moduli near the theoretical calculation for an intercalated and partial exfoliated system. This indicates that the nanocomposites are beginning to exfoliate. A 100 m.eq. quaternary ammonium exchange level was used for all subsequent surface treatment because it had the largest increase in storage modulus and was shown to be the optimum surface exchange capacity.

| <i>Clay Treatments<br/>Sample I.D.</i> | <i>Storage Modulus at 50° C<br/>(MPa)</i> |
|--|---|
| <b>Quaternary Amine 2HT (m.eq.)</b>    |   |
| 90                                     | 32.15                                     |
| 95                                     | 39.03                                     |
| 100                                    | 42.50                                     |
| 105                                    | 40.36                                     |
| 110                                    | 32.76                                     |

**Table 1: This table represents the storage modulus at 50° C for the quaternary ammonium series nanocomposites.**

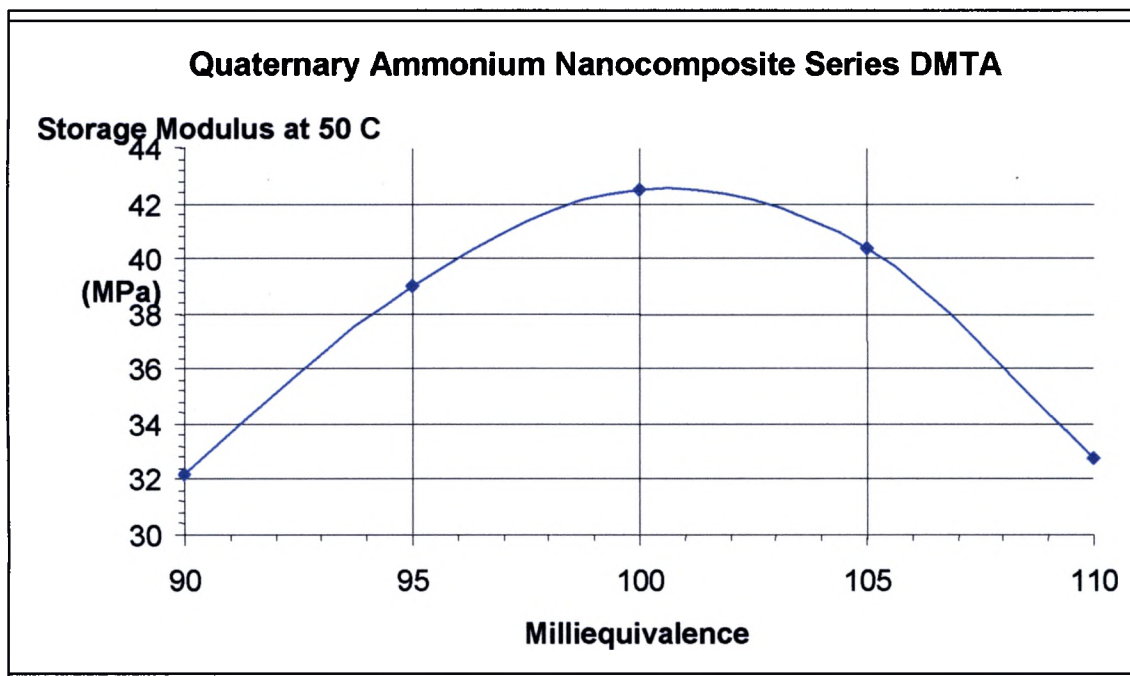


**Figure 16: A graphical representation of the increasing modulus with increasing milliequivalence.**

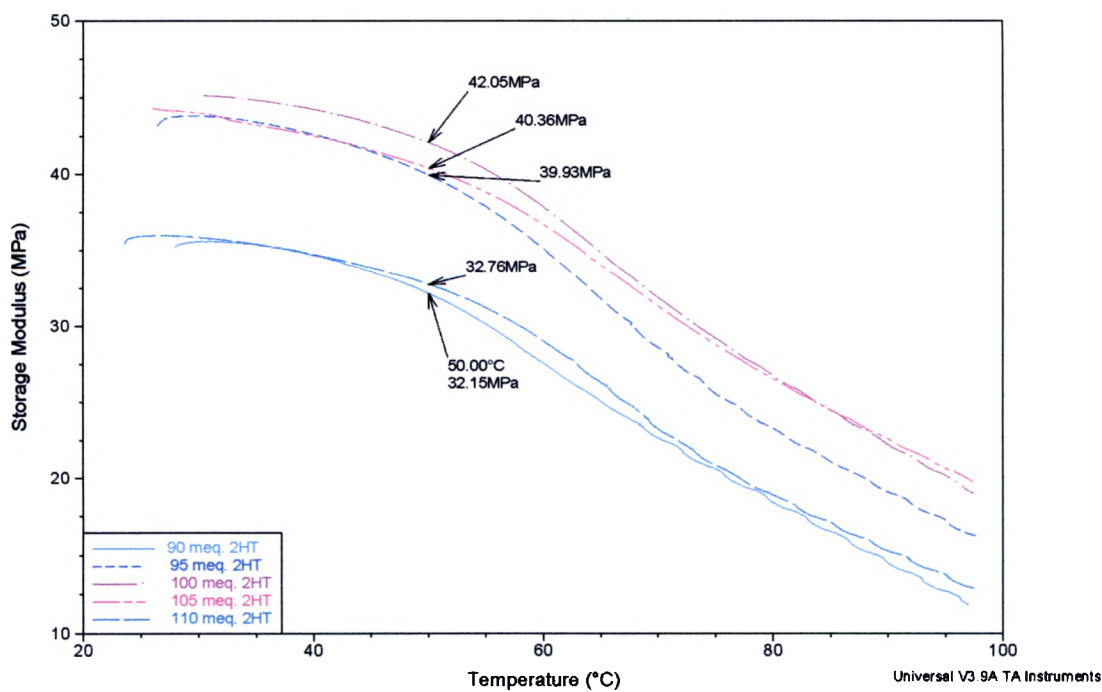


**Figure 17: DMTA for the 2HT quaternary ammonium ladder series of milliequivalence.**

### 3.1.2 Surface Sorption Polymer Treatment Clay-polymer Nanocomposites

The partial negative charge near the surface of the clay by the exchange of aluminum and magnesium in the octahedral layer of the clay hinders the exfoliation process due to polarity. A surface sorption treatment was used to examine the effect that the excess charge would play on exfoliation. The polymer surface sorption treatment on the clay acts as a buffer to lessen the effect of the slightly negative charge near the clay's surface. Table 2 and table 3 represent the storage modulus of PVP and PPG at 50 °C treated clay-polyurethane composite.

| <i>Clay Treatments<br/>Sample I.D.</i> | <i>Storage Modulus at 50° C<br/>(MPa)</i> |
|--|---|
| <b>PVP (%) 90 m.eq.2HT (200 mesh)</b>  |   |
| 2% PVP                                 | 35.48                                     |
| 4% PVP                                 | 28.18                                     |
| 6% PVP                                 | 32.70                                     |

**Table 2: Storage modulus for PVP surface treatment nanocomposite**

| <i>Clay Treatments<br/>Sample I.D.</i> | <i>Storage Modulus at 50° C<br/>(MPa)</i> |
|--|---|
| <b>PPG (%) 100m.eq.2HT</b>             |   |
| 2% PPG (200 mesh)                      | 37.96                                     |
| 2% PPG (325 mesh)                      | 36.48                                     |
| 4% PPG (200 mesh)                      | 46.71                                     |
| 4% PPG (325 mesh)                      | 48.83                                     |
| 6% PPG (200 mesh)                      | 43.80                                     |
| 6% PPG (325 mesh)                      | 37.12                                     |

**Table 3: Storage modulus for PPG surface treatment nanocomposites**

The PVP and PPG were mixed with the clay at 2, 4, and 6 % by weight of the clay (figure 18 and 19). The figure 18 indicates that the PPG at both 200 mesh and 325 mesh displayed an optimization peaks. The 4% PPG gave the highest storage modulus for both the 200 and 325 mesh (figure 20). The lowest storage modulus for PVP was shown by

the 4% sample. The PVP hindered the exfoliation process, while the PPG increased the storage modulus 205 % compared to the pristine polymer and 14.9 % increase compared to the best quaternary ammonium treatment. The increase in storage modulus compared to the clay-polymer nanocomposite, with just the surface treatment, indicates that the PPG is helping the exfoliation/intercalation of the nanocomposite. The system is however, still in the theoretical range of intercalated system. The PVP actually seems to decrease the storage modulus since the PVP is hydrophilic and the Pellethane is hydrophobic. PPG did however, increased the storage modulus compared to PVP. This is attributed to the hydrophobic nature of PPG. It is expected to be more compatible with the Pellethane, and this is supported by the storage modulus increase.

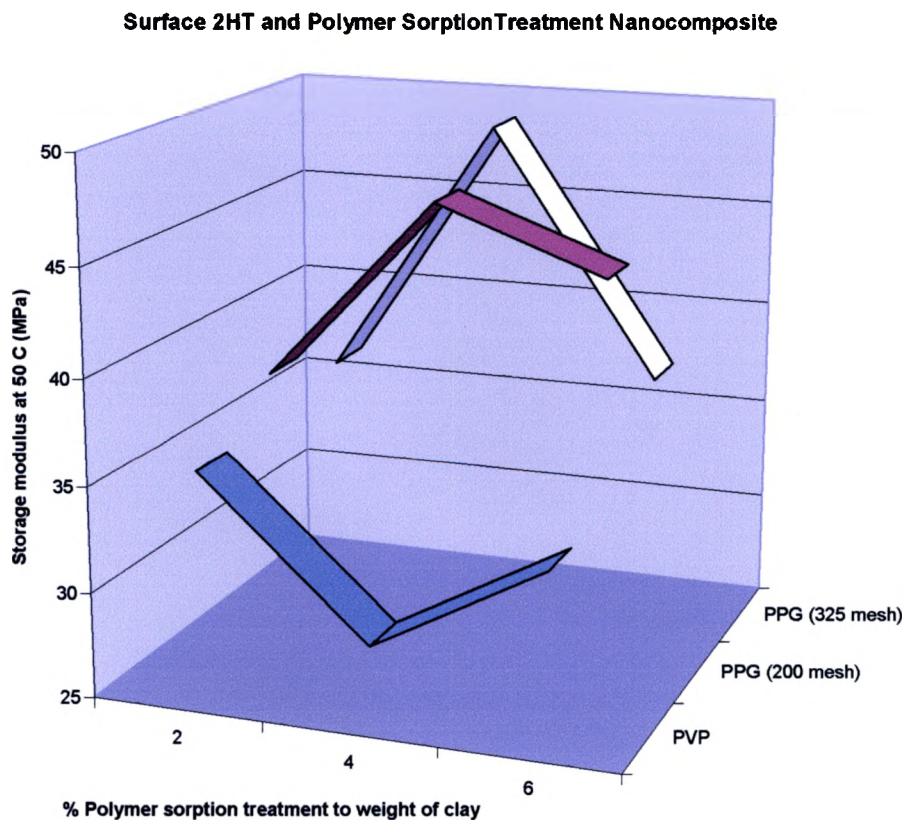


**Figure 18: Graphical representations of the different polymer surface treatments with respect to the storage modulus.**

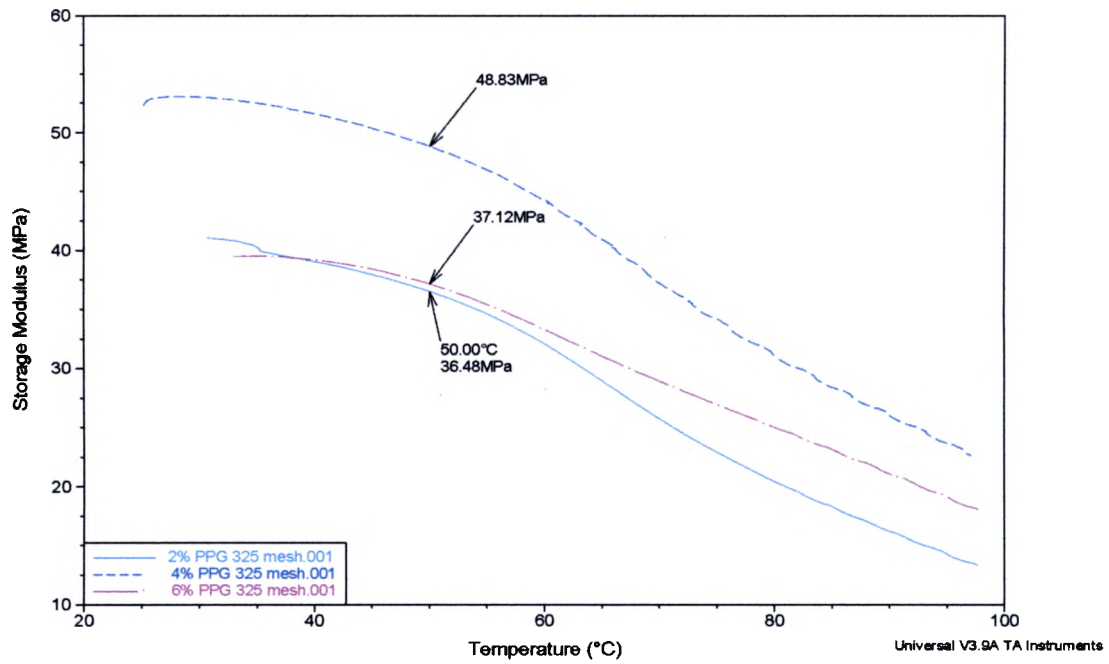


**Figure 19: DMTA for the ladder series of PPG at 2, 4, and 6% 325 mesh.**

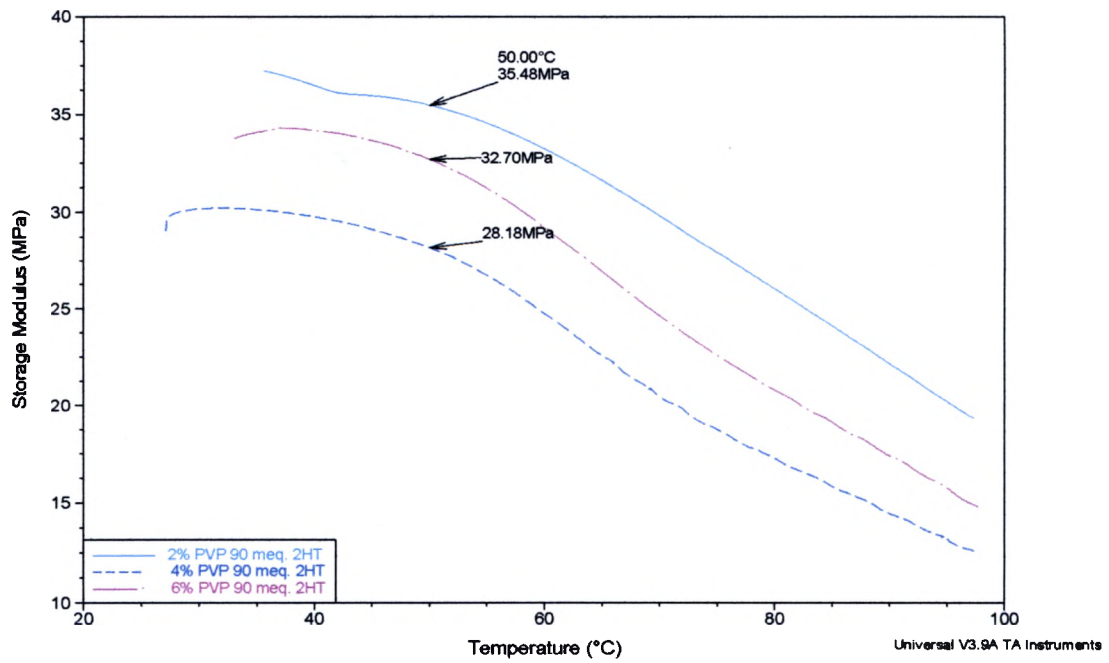


**Figure 20: DMTA for the ladder series of PVP at 2, 4, and 6 %.**

### 3.1.3 Edge, Surface Sorption, and Surface Treated Clay-polymer Nanocomposites

Clays were produced with 100 m.eq. 2HT, 2% PPG, and various silane coupling agents. The clays were compounded into polyurethane and evaluated by DMTA. The storage modulus for each edge-treated clay was higher than the storage modulus of the surface sorption clay at 2% PPG (table 4). All of the storage moduli for the clay-polymer nanocomposites were within the theoretical range predicted by HALPIN-TSAI, which would indicate that intercalation had occurred with some exfoliation. The 200 mesh outperformed the 325 mesh clay in all systems except vinyltrimethoxy silane (figures 21 and 22) system. The 3-aminotrimethoxy silane treatment had the highest increase in storage modulus at 164 % of the value for the pristine polymer. 3-Aminopropyltrimethoxy silane also had a 15.5 % increase compared to the 2% PPG clay nanocomposite. The clays were treated with 2% PPG, rather than the optimum 4% , because the clays were made before the results were obtained for the PPG ladder series. Octadecyltrimethoxy silane and 3-aminopropyltrimethoxy silane were selected to be used for the remainder of the testing.

| <i>Clay Treatments<br/>Sample I.D.</i>   | <i>Storage Modulus at 50° C<br/>(MPa)</i> |
|--|---|
| <b>Edge Treatment 2%PPG 100m.eq. 2HT</b> |   |
| 3-Aminotrimethoxy Silane (200mesh)       | 42.15                                     |
| 3-Aminotrimethoxy Silane (325mesh)       | 30.86                                     |
| Dodecyltrimethoxy Silane (200mesh)       | 39.98                                     |
| Dodecyltrimethoxy Silane (325mesh)       | 41.39                                     |
| Octadecyltrimethoxy Silane (200mesh)     | 37.41                                     |
| Octadecyltrimethoxy Silane (325mesh)     | 33.56                                     |
| Phenyltrimethoxy Silane (200mesh)        | 39.71                                     |
| Phenyltrimethoxy Silane (325mesh)        | 33.47                                     |
| Vinyltrimethoxy Silane (200mesh)         | 30.56                                     |
| Vinyltrimethoxy Silane (325mesh)         | 40.74                                     |

**Table 4: Storage modulus for edge treated nanocomposites at 200 mesh and 325 mesh.**

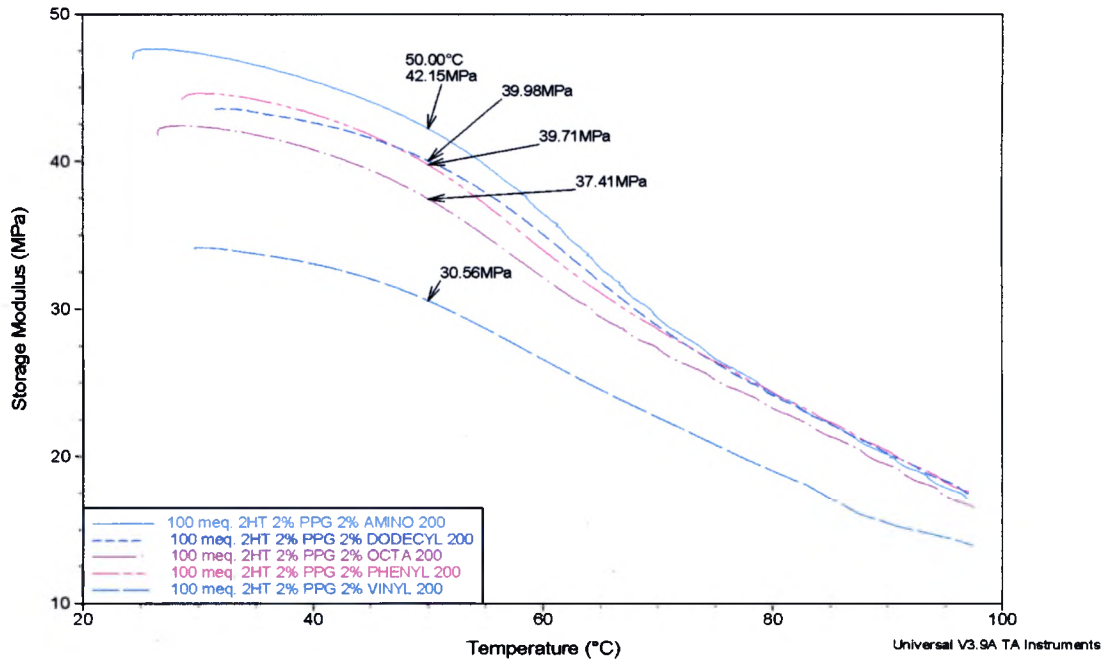


Figure 21: DMTA for the edge, PPG, and 2HT treated clay at 200 mesh.

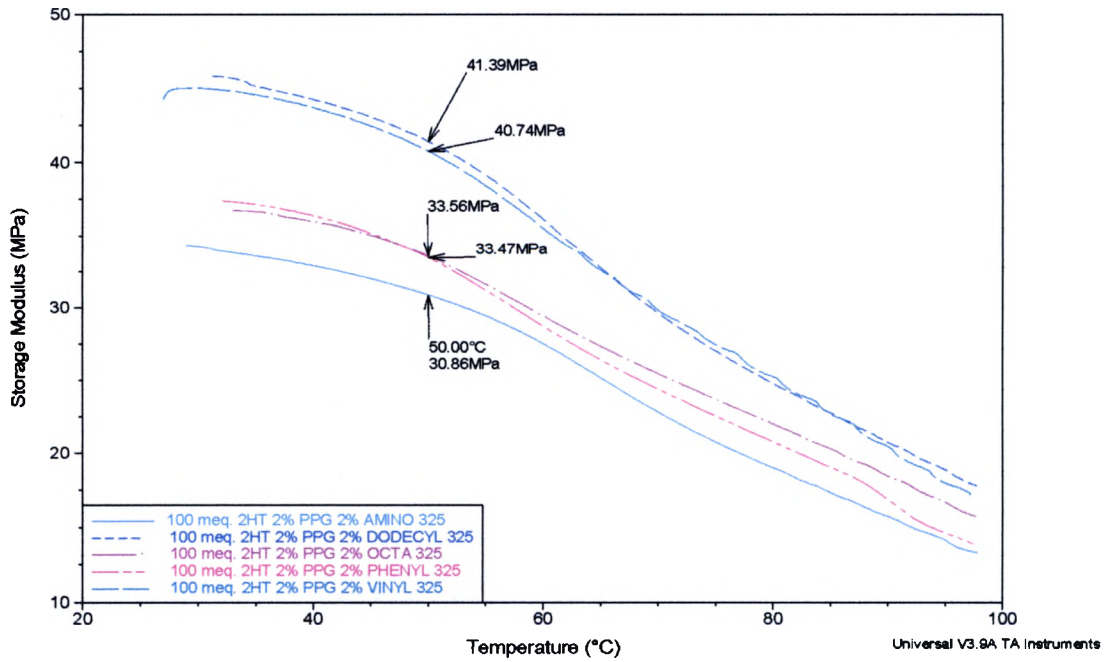


Figure 22: DMTA for the edge, PPG, 2HT treated clay at 325 mesh.

### 3.1.4 Edge and Quaternary Ammonium Treated Clay-polymer Nanocomposite

The nanocomposites which were treated at the surface and the edge, with no sorption treatment on the clay (table 5), showed no unusual increase in the storage modulus compared to other nanocomposites (figure 23). The storage modulus for 3-aminopropyltrimethoxy silane lowered without the PPG treatment, while the octadecyltrimethoxy silane increased the modulus slightly without the PPG treatment. The octadecyltrimethoxy silane without PPG increased the storage modulus by 10.6 % and 21 % for the 200 mesh and 325 mesh, respectively.

| <i>Clay Treatments<br/>Sample I.D.</i>  | <i>Storage Modulus at 50° C<br/>(MPa)</i> |
|---|---|
| <b>100 m.eq. 2HT and Edge Treatment</b> |   |
| 3-Aminotrimethoxy Silane (200mesh)      | 33.84                                     |
| 3-Aminotrimethoxy Silane (325mesh)      | 34.89                                     |
| Octadecyltrimethoxy Silane (200mesh)    | 41.36                                     |
| Octadecyltrimethoxy Silane (325mesh)    | 40.6                                      |

**Table 5 Storage modulus for edge and surface treated clay-polymer nanocomposite.**

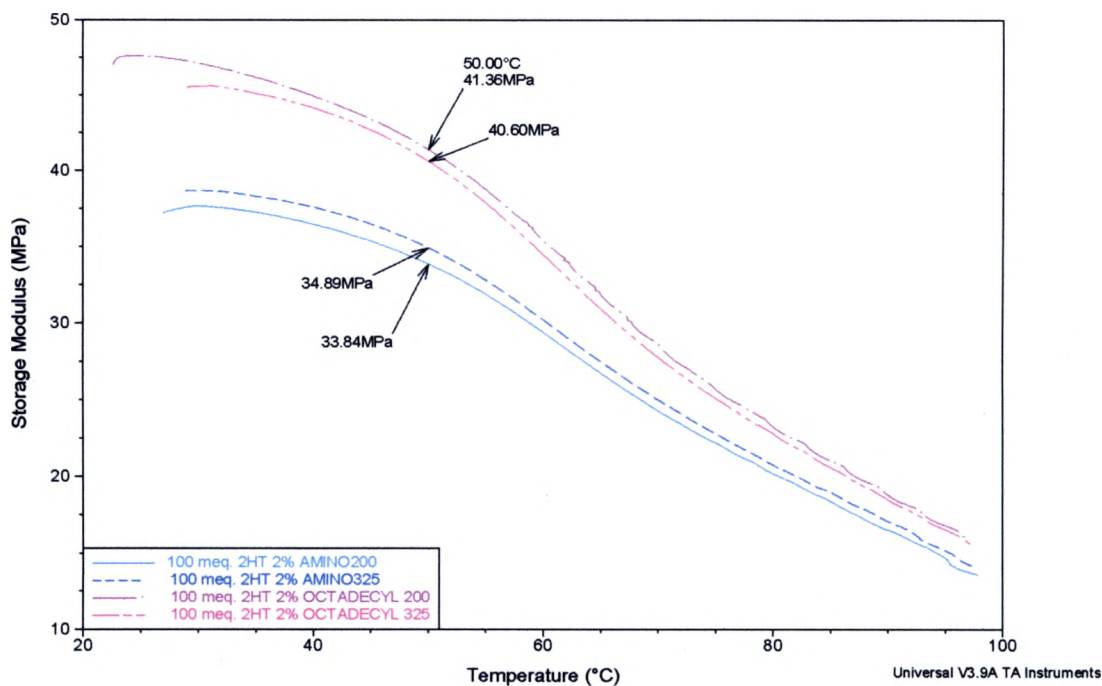


**Figure 23: DMTA of the edge and 2HT treated clay nanocomposite.**

### 3.1.5 Edge and Surface Sorption Treated Clay-polymer Nanocomposites

The storage modulus was measured for nanocomposites that had both the edge and surface sorption treatments, but no quaternary ammonium treatment on the clay (table 6 and figure 24)). Both the 3-aminotrimethoxy silane and the octadecyltrimethoxy silane with 2% PPG had similar results as the clay with just the edge and quaternary ammonium surface treatment. The storage modulus increased slightly for both nanocomposites. The samples were opaque with visible partials of clay throughout the matrix, which indicated that a macroscale composite was formed.

| <i>Clay Treatments<br/>Sample I.D.</i> | <i>Storage Modulus at 50° C<br/>(MPa)</i> |
|--|---|
| <b>2% PPG and Edge Treatment</b>       |   |
| 3-Aminotrimethoxy Silane (325mesh)     | 35.99                                     |
| Octadecyltrimethoxy Silane (325mesh)   | 41.46                                     |

**Table 6: Storage modulus for the surface sorption and edge treated clay-polymer nanocomposite.**

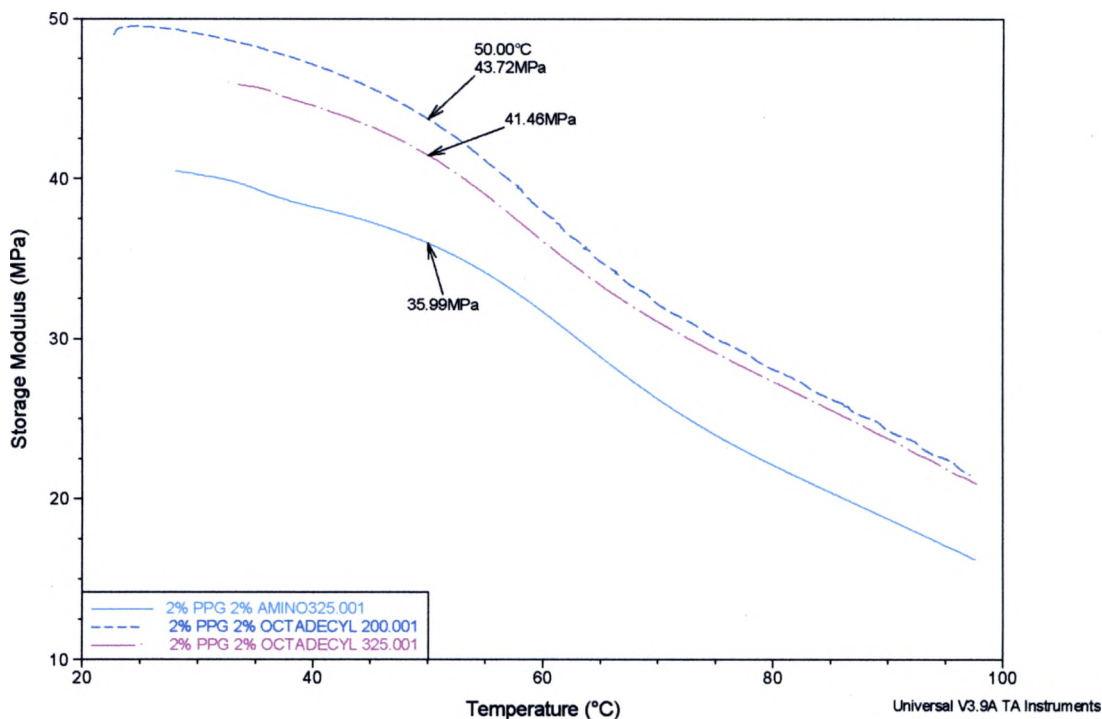


**Figure 24: DMTA of the edge and surface sorption (PPG) clay nanocomposite.**

### 3.1.6 Washed Clay-polymer Nanocomposites

The washed nanocomposites had all three treatments and were also washed three times to remove any excess sodium ions from the clay in order to determine if the excess sodium ions had an effect on the storage modulus. The grinding and sieving was not needed when the clay was washed because the clay was already a fine powder. The powder was brushed slightly to loosen the clay platelets. The storage modulus increased significantly for the 3-aminotrimethoxy silane, 2% PPG, and 100 m.eq. 2HT washed clay compared to the same clay when it was not washed (table 7 and figure 25). Relative to the highest storage modulus for the 3-aminotrimethoxy silane, the increase was 23.8 %. The increase in storage modulus for the 3-aminotrimethoxy silane, 2% PPG, and 100

m.eq. 2HT washed clay came closest to the high end of the theoretical prediction, which indicated that the specific combination approached an exfoliated nanocomposite.

| <i>Clay Treatments<br/>Sample I.D.</i>                      | <i>Storage Modulus at 50° C<br/>(MPa)</i> |
|---|---|
| Washed 100 m.eq. 2HT  | 35.12                                     |
| Washed 100 m.eq. 2HT 2% PPG                                 | 45.50                                     |
| <b>Washed 100 m.eq. 2HT, 2% PPG, and<br/>Edge Treatment</b> |   |
| 3-Aminotrimethoxy Silane                                    | 52.20                                     |
| Octadecyltrimethoxy Silane                                  | 39.38                                     |

**Table 7: Storage modulus for the washed quaternary ammonium surface treated, PPG treated, and edge treated clay-polymer nanocomposite.**

The washed 100 m.eq. 2HT clay did not have an effect on the storage modulus compared to the same unwashed clay-polymer nanocomposite. Also, the washed 100 m.eq. 2HT, 4% PPG clay-polymer and the octadecyltrimethoxy silane, 2% PPG, 100.m.eq 2HT clay did not have a significant increase in storage modulus once the clay was washed. Therefore, the that the washing only increased the storage modulus of the 3-aminopropyltrimethoxy silane clay possibly because the amino functional group interacted with the sodium ions left in the clay due to the polarity of both the amino group and the sodium ions.

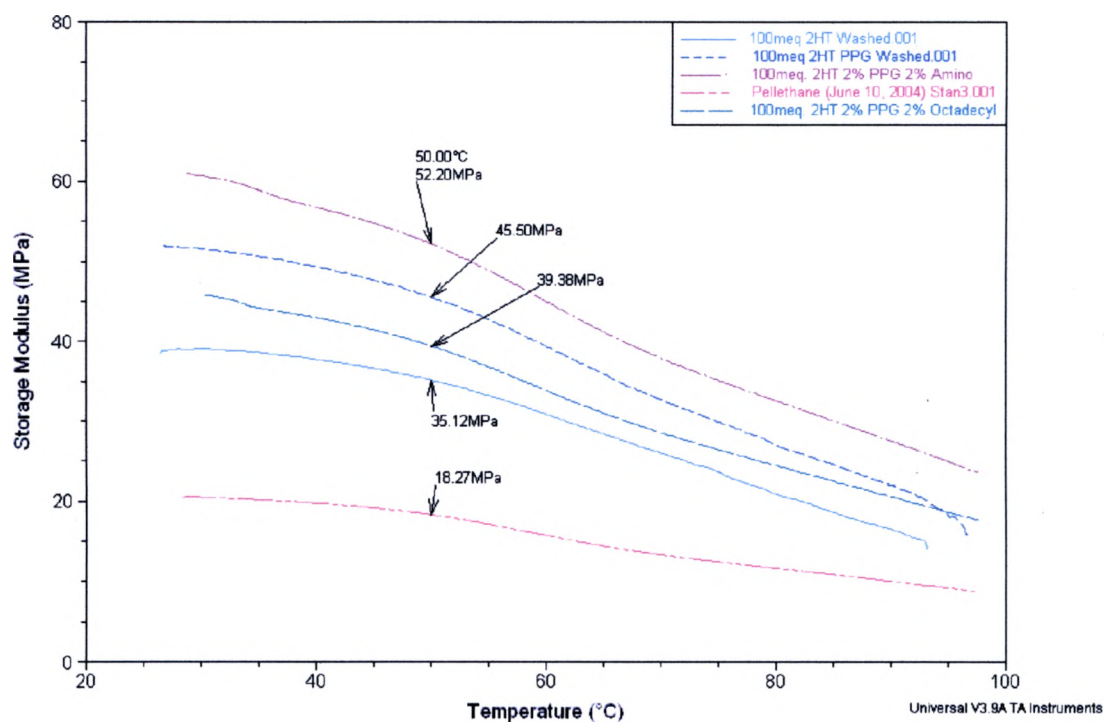


**Figure 25: DMTA of washed clay nanocomposites.**

### 3.2 Tensile Testing

Tensile properties are one of the most frequently considered, evaluated, and used throughout the polymer industry. The properties are an important indicator of the material's behavior under load or a given force, such as tension. Tensile testing provides useful data such as tensile yield strength, tensile strength at break (ultimate tensile strength), tensile modulus (Young's modulus), and elongation at yield and break. Figure 26 represents a typical stress-strain curve from tensile testing.

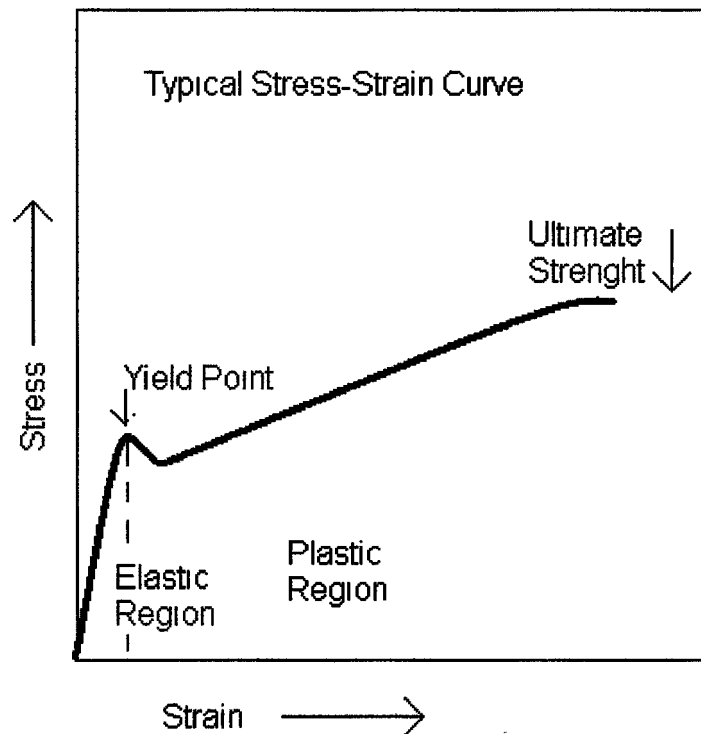


**Figure 26: Typical stress-strain curve for a tensile test.**

The Young's Modulus is the ratio of stress to strain within the elastic region of the stress-strain curve. The shape of the curve can illustrate the material's behavior. If the initial slope is large and fails with little strain, then the material is more likely to be hard and brittle. On the other hand if the slope is very small initially and withstands large strain, the material is more likely to be soft and tough. The stress-strain curve can also indicate whether or not the overall material is tough. The area under the curve (MPa) is the measure of the material's toughness. The greater the area, the tougher the material is, and the more energy it will take to break it.

Each nanocomposite was tested to determine tensile modulus, yield point, and peak load. The tensile modulus (Young's modulus) describes the ratio of stress to strain in the

elastic region of the stress-strain curve. For the pristine polymer, the Young's modulus is  $15.75 (\pm 3.24) \text{ N/mm}^2$ , which indicates that the pristine polymer is a soft and tough material (figure 27). Yield point is also an important factor because it shows when the applied strain exceeds the elastic limit. The polyurethane doesn't exhibit true elastomeric behavior with regards to yield point. The slope changes to give a more linear ratio between the stress and strain. The peak load is the ultimate tensile strength which is the amount of stress the polymer can take before failing. The pristine polymer did not have a peak load because the grips released the polymer before it failed. The test was repeated two more times to ensure the polymer would not fail. Figure 27 is the stress-strain curve for the pristine polymer.

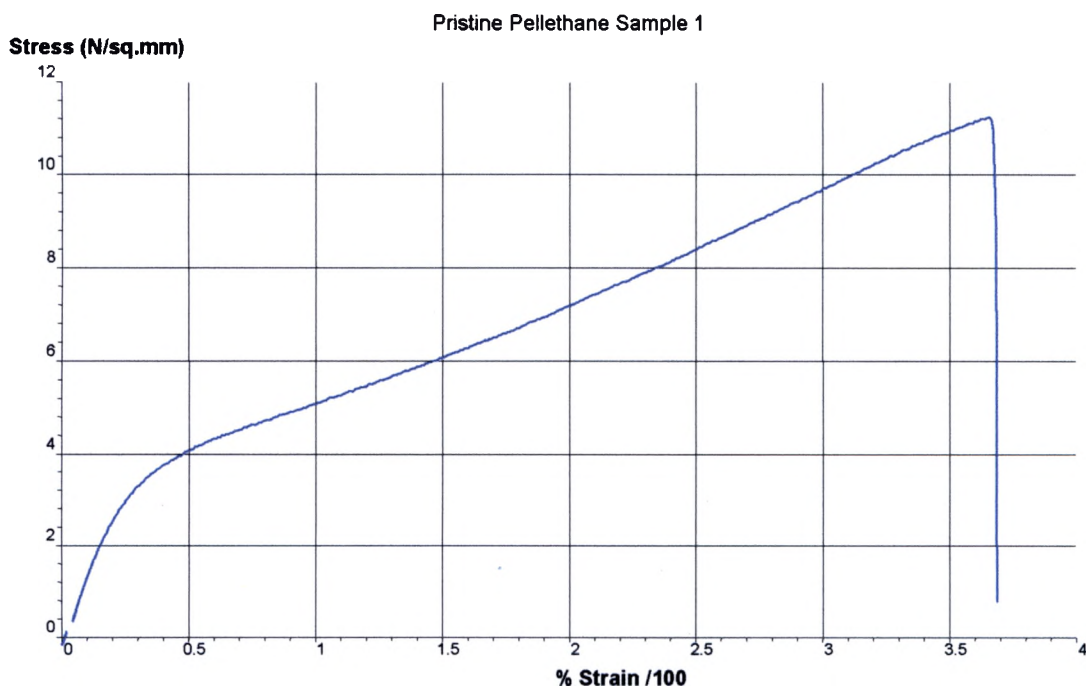


**Figure 27: Stress-strain curve for the pristine polymer.**

### 3.2.1 Optimized Series with all 3 Treated Clay-polymer Nanocomposites

Table 8 depicts the Young's modulus, yield point, and peak load (ultimate tensile strength) for the optimized series of clay-polymer nanocomposites. Young's modulus increased by at least 50% compared to the pristine polymer for all polymer-clay nanocomposites. The largest increase in the Young's modulus was the 100 m.eq. 2HT 4% PPG 2% 3-aminotrimethoxy silane (325 mesh) polymer-clay nanocomposite (figure 28) with an increase of 96.7%. The doubling of the Young's modulus is characterized by an increase in slope and this indicates that the material is stiffer or requires more energy for deformation in the elastic region when compared to the pristine polymer. The 100 m.eq. 2HT 4% PPG 2% 3-aminotrimethoxy silane (325 mesh) clay-polymer nanocomposite also had the highest increase in yield point with a 32 % increase. The increase in the yield point indicates the nanocomposite can withstand more stress in the elastic region than the pristine polymer. The yield point was calculated by extrapolating the initial slope and the more linear second slope and determining where the two lines intersect. The 100 m.eq. 2HT polymer-clay nanocomposite and the 100 m.eq. 2HT 2% PPG 2% octadecyltrimethoxy silane (200 mesh) also performed well with a 27% increase in the yield point. The 100 m.eq. 2HT 2%PPG 2% octadecyltrimethoxy silane (200 mesh) polymer-clay nanocomposite would likely have performed better if the PPG was increased to 4% as the 100 m.eq. 2HT 4% PPG 2% 3-aminotrimethoxy silane (325 mesh) polymer-clay nanocomposite.

| <i>Clay Treatment<br/>Sample I.D.</i>                       | <i>Young's<br/>Modulus<br/>(N/sq. mm)</i> | <i>Yield Point (N)</i> | <i>Peak Load (N)</i> |
|---|---|------------------------|----------------------|
| Pure Pellethane   | 15.75 ( $\pm$ 3.24)                       | 3.15 ( $\pm$ 0.071)    | No Break             |
| 100 m.eq. 2HT   | 30.74 ( $\pm$ 2.93)                       | 4.01 ( $\pm$ 0.69)     | 117.2 ( $\pm$ 32.1)  |
| 100 m.eq. 2HT 4% PPG 200 mesh                               | 24.07 ( $\pm$ 1.47)                       | 3.34 ( $\pm$ 0.40)     | 85.0 ( $\pm$ 45.4)   |
| 100 m.eq. 2HT 4% PPG 325 mesh                               | N/A                                       | N/A                    | N/A                  |
| 100 m.eq. 2HT 2% PPG 2% 3-Aminotrimethoxy Silane 200 mesh   | 26.54 ( $\pm$ 1.70)                       | 3.64 ( $\pm$ 0.39)     | 120.4 ( $\pm$ 25.8)  |
| 100 m.eq. 2HT 2% PPG 2% 3-Aminotrimethoxy Silane 325 mesh   | 23.47 ( $\pm$ 1.83)                       | 3.46 ( $\pm$ 0.74)     | 117.0 ( $\pm$ 46.8)  |
| 100 m.eq. 2HT 2% PPG 2% Octadecyltrimethoxy Silane 200 mesh | 26.01 ( $\pm$ 2.04)                       | 4.05 ( $\pm$ 0.66)     | 143.7 ( $\pm$ 59.3)  |
| 100 m.eq. 2HT 2% PPG 2% Octadecyltrimethoxy Silane 325 mesh | 23.61 ( $\pm$ 0.90)                       | 3.38 ( $\pm$ 0.37)     | 118.6 ( $\pm$ 30.7)  |
| 100 m.eq. 2HT 4% PPG 3-Aminotrimethoxy Silane 200 mesh      | 25.55 ( $\pm$ 0.709)                      | 3.55 ( $\pm$ 0.21)     | 134.9 ( $\pm$ 16.8)  |
| 100 m.eq. 2HT 4% PPG 3-Aminotrimethoxy Silane 325 mesh      | 30.98 ( $\pm$ 1.33)                       | 4.16 ( $\pm$ 0.62)     | 155.2 ( $\pm$ 41.5)  |

**Table 8: Tensile properties for the optimized series of the clay/polymer nanocomposite.**

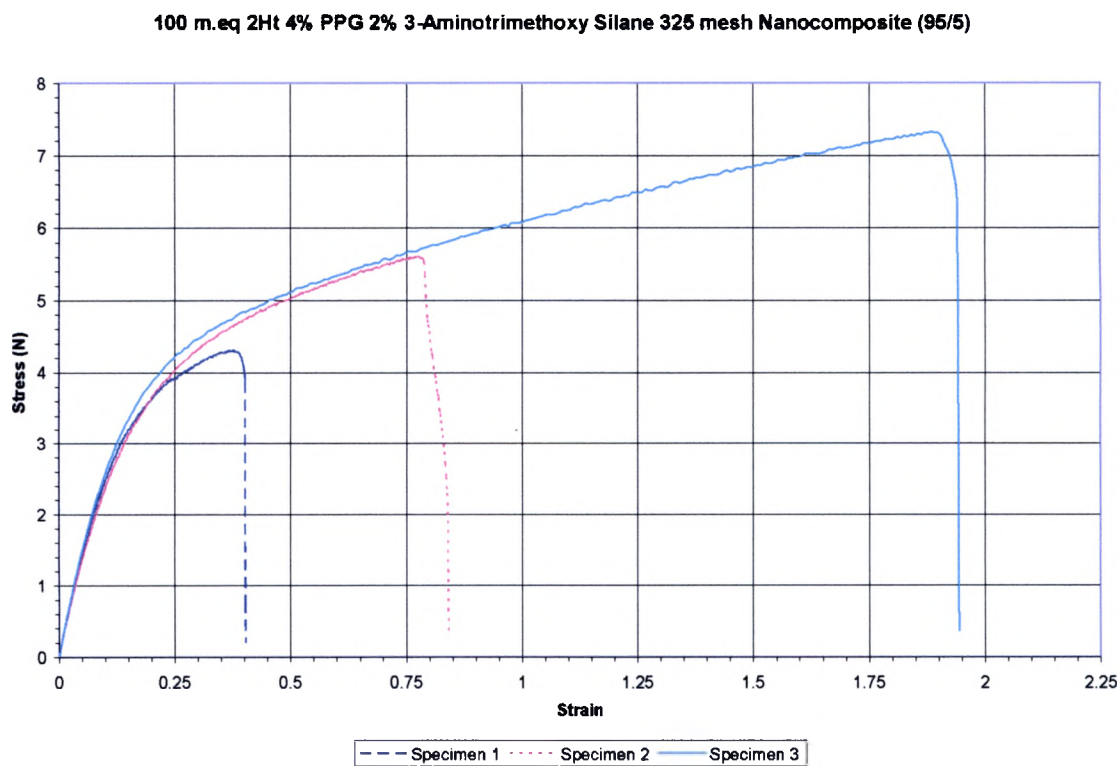


**Figure 28: Stress-strain curve for 100 m.eq. 2HT 4% PPG 2% 3-aminotrimethoxy silane (325 mesh) nanocomposite. The variance is due to the processing techniques.**

The pristine polymer performed better than the nanocomposites in terms of peak load. Each of the polymer-clay nanocomposites failed, while the pristine polymer did not fail. The peak load of the pristine polymer could not be calculated because the polymer slipped from the grips. The nanocomposites may have failed because each sample was compression molded and then cut with a tensile bar cutter which created a layering or laminate effect due to the clay being intercalated and not completely exfoliated in the system. Compression molding heats the outer surface of the material longer than the interior, which in this case, allows the clay platelets to align due to compression on the outer edges in the polymer matrix. If the nanocomposites were injection molded the laminate effect would not have had as large an effect and the peak load would increase. The lamination effect is illustrated in figure 29 for the 100 m.eq 2HT polymer-clay nanocomposite. The stress-strain curves fractures in 5 places before it completely breaks or fails. All of the samples displayed this effect to varying degrees, contributing to the high variability seen in figure 28. The lamination effect could also be the reason that the tensile modulus appeared to be a poor indicator of exfoliation.

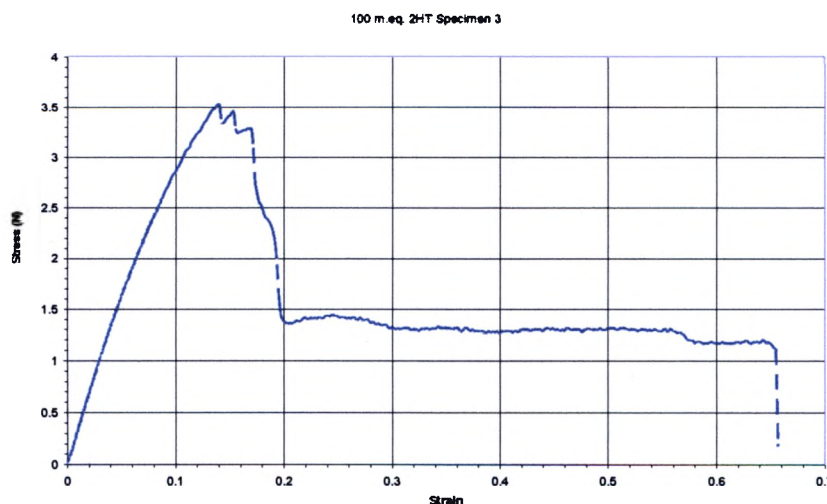


**Figure 29: Stress-strain curve for 100 m.eq. 2HT clay-polymer nanocomposite specimen 3.**

### 3.2.2 Edge and Quaternary Ammonium Treated Clay-polymer Nanocomposites

The Young's modulus, yield point, and peak load for the polymer-clay nanocomposites treated with the quaternary ammonium 2HT and silane are represented in Table 9. The nanocomposites displayed similar results (figure 30) to the clay-polymer nanocomposites with all three treatments. The only difference is that the yield point increased more than that of the previous nanocomposites. The 100 m.eq. 2HT 2% octadecyltrimethoxy silane (325 mesh) clay-polymer nanocomposite had the largest increase (38.7 %) compared to the pristine polymer. Each of the nanocomposites also failed at a given peak load due to the laminating effect previously described.

| <i>Clay Treatment<br/>Sample I.D.</i>                   | <i>Young's<br/>Modulus<br/>(N/sq. mm)</i> | <i>Yield Point (N)</i> | <i>Peak Load (N)</i> |
|---|---|------------------------|----------------------|
| 100 m.eq. 2HT 2% 3-Aminotrimethoxy<br>Silane 200 mesh   | 26.15 (± 1.60)                            | 4.23 (± 0.62)          | 129.6 (± 44.8)       |
| 100 m.eq. 2HT 2% 3-Aminotrimethoxy<br>Silane 325 mesh   | 24.71 (± 0.582)                           | 4.18 (± 0.27)          | 124.6 (± 7.24)       |
| 100 m.eq. 2HT 2% Octadecyltrimethoxy<br>Silane 200 mesh | 26.96 (± 1.48)                            | 2.63 (± 0.52)          | 76.67 (± 15.4)       |
| 100 m.eq. 2HT 2% Octadecyltrimethoxy<br>Silane 325 mesh | 27.92 (± 0.402)                           | 4.37 (± 0.042)         | 140.8 (± 11.3)       |

**Table 9: Tensile data for the quaternary ammonium and edge treated clay-polymer nanocomposite.**

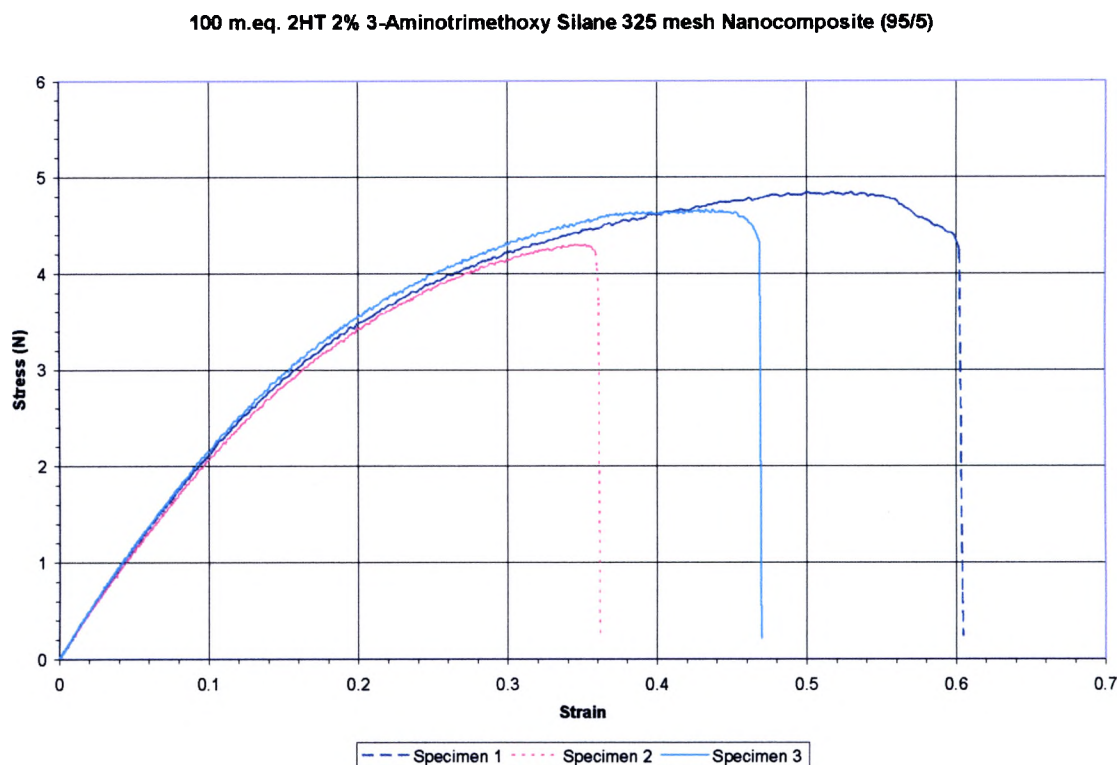


**Figure 30: Stress-strain curve for 100 m.eq. 2HT 2% 3-aminotrimethoxy silane nanocomposite.**

### 3.2.3 Edge and PPG Treated Clay-polymer Nanocomposites

Table 10 contains the tensile data for the clay-polymer nanocomposites with the silane edge treatment and the PPG surface sorption treatment. The nanocomposites did not have the 2HT quaternary ammonium treatment, but they had similar Young's moduli as the nanocomposites with all three treatments. They did however, exhibit very different peak loads. The nanocomposites did not display the laminating effect previously discussed due to the macrocomposites of clay in the polymer matrix. The 2% PPG 2% 3-Aminotrimethoxy Silane 325 mesh and the 2% PPG 2% Octadecyltrimethoxy Silane 325 mesh (figure 31) polymer-clay nanocomposites did not fail. They displayed the resistance to break. The 2% PPG 2% octadecyltrimethoxy silane 200 mesh did however

fail in 2 of the 3 samples. Failure was most likely due to tiny fractures in the samples themselves before the testing took place, but they still had the largest peak load out of the remaining nanocomposites.

The nanocomposites with only the PPG and silane edge treatment did not display a peak load. As previously mentioned, the composites are opaque due to large clay particles in the polymer matrix. The large particles indicate that they are not distributed in the polymer matrix on the nanolevel, but on the macro scale level and are macrocomposite rather than nanocomposites. Macrocomposites may have some clay platelets distributed on the nanolevel, but the majority of the clay is visible to the naked eye.

Macrocomposite can increase the Young's modulus and the yield point without the loss of peak load, but macrocomposites do not have the same clarity as a nanocomposite nor do they give as high of a modulus as an exfoliated nanocomposite. There are advantages to having macrocomposites, but nanocomposite theoretically will give better overall properties.

| <i>Clay Treatment<br/>Sample I.D.</i>            | <i>Young's<br/>Modulus<br/>(N/sq. mm)</i> | <i>Yield Point (N)</i> | <i>Peak Load (N)</i> |
|--|---|------------------------|----------------------|
| 2% PPG 2% 3-Aminotrimethoxy Silane<br>200 mesh   | N/A                                       | N/A                    | N/A                  |
| 2% PPG 2% 3-Aminotrimethoxy Silane<br>325 mesh   | 32.41 ( $\pm$ 1.30)                       | 4.75 ( $\pm$ 0.05)     | No Break             |
| 2% PPG 2% Octadecyltrimethoxy Silane<br>200 mesh | 26.82 ( $\pm$ 2.28)                       | 4.54 ( $\pm$ 0.13)     | 330.6 ( $\pm$ 123)   |
| 2% PPG 2% Octadecyltrimethoxy Silane<br>325 mesh | 24.43 ( $\pm$ 1.41)                       | 4.02 ( $\pm$ 0.19)     | No Break             |

**Table 10: Tensile data for the clay-polymer nanocomposites without any 2HT**

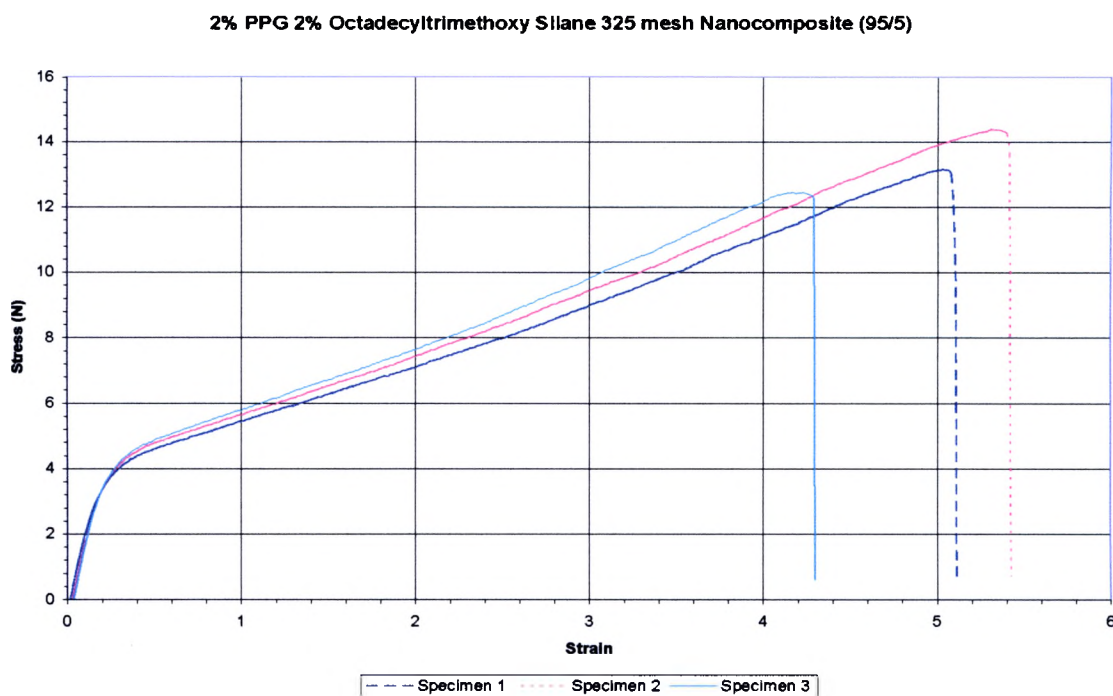


**Figure 31: Stress-strain curve for 2% PPG 2% octadecyltrimethoxy Silane 325 mesh nanocomposite.**

### 3.2.4 Washed Clay-polymer Nanocomposites

Table 11 contains the Young's Modulus, yield point, and peak load for the washed nanocomposites with one or more of the clay treatments. The nanocomposites did not show any drastic increase in tensile properties as compared to their unwashed counterparts. The Young's modulus, yield point, and peak load all fall within the standard deviation of the corresponding nanocomposite without washing. Washing the sodium ions out of the clay before processing has no effect on the physical properties.

| <i>Clay Treatment<br/>Sample I.D.</i>                        | <i>Young's<br/>Modulus<br/>(N/sq. mm)</i> | <i>Yield Point (N)</i> | <i>Peak Load (N)</i> |
|--|---|------------------------|----------------------|
| Washed 100 m.eq. 2HT   | 28.73 (± 2.07)                            | 2.96 (± 0.78)          | 82.4 (± 25.3)        |
| Washed 100 m.eq. 2HT 4% PPG                                  | 26.36 (± 0.986)                           | 4.50 (± 0.29)          | 151.8 (± 1.25)       |
| Washed 100 m.eq. 2HT 2% PPG 2% 3-<br>Aminotrimethoxy Silane  | 26.16 (± 0.999)                           | 2.30 (± 0.28)          | 49.8 (± 20.29)       |
| Washed 100 m.eq. 2HT 2% PPG 2%<br>Octadecyltrimethoxy Silane | 27.04 (± 0.529)                           | 3.14 (± 0.61)          | 120.0 (± 50.0)       |

**Table 11: Tensile data for the washed series of nanocomposites**

### 3.3 X-ray Diffraction Results

The various systems were tested by X-Ray diffraction (XRD). XRD is used to determine the degree of exfoliation of organoclays in the polymer matrix. As the organoclay disperses into the polymer matrix, the distance between the silicate layers grows. The separation between the layers is represented by the changing position of the peaks in the XRD diagram (figure 32) [12]. Bragg's law, below, is used

$$n*\lambda = 2*d*\sin \theta$$

where n is an integer indication peak number

$\lambda$  is the wavelength of the x-ray

d is the spacing between the clay layers

$\theta$  is the angle of incidence of the x-ray beam [12].

to relate the relationship between the incident radiation and the layer spacing.

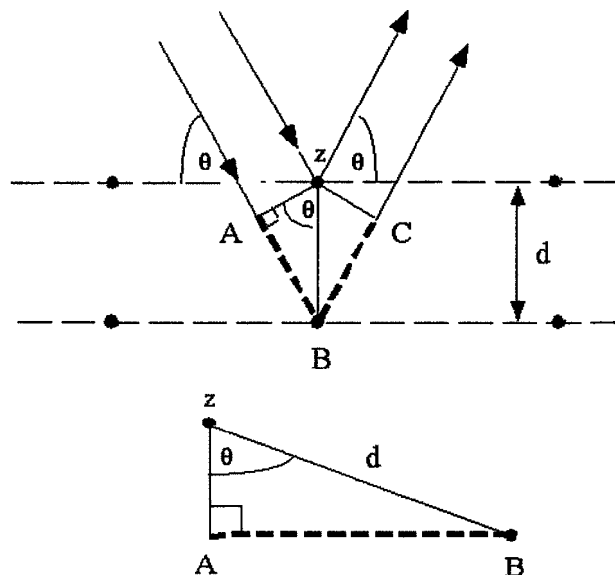


**Figure 32: XRD diffraction peak derivation**

The Basal spacing (d-spacing) can be calculated from the diffraction peak on the x-ray graph [3]. A well intercalated system will show very ordered peaks on the XRD, but a completely exfoliated system will show no coherent scattering and, as a result, no peaks in the diffraction pattern.

Each diffraction pattern was evaluated and the first peak, in degrees, was converted into Basal spacing using Bragg's law. The following tables list all of the d-spacings which correlate to the first order diffraction peaks for the given nanocomposite. As expected, the pure Pellethane did not show a diffraction peak within the 2-20 2-theta-omega scan (figure 33). The amorphous polymer simply scatters the X-rays in all directions.

The sodium montmorillonite clay without any treatment shows a diffraction peak at  $9.2^\circ$  and  $7.1^\circ$  ( $2\theta$ ), which corresponds to a d-spacing  $12.5 \text{ \AA}$ . The d-spacing of in montmorillonite is due to the hydration of the silica sheets. The thickness of the clay

platelet is 9.6 Å, and the gallery of the clay, which is calculated as the d-spacing minus the thickness of the clay, is only about 3 Å.

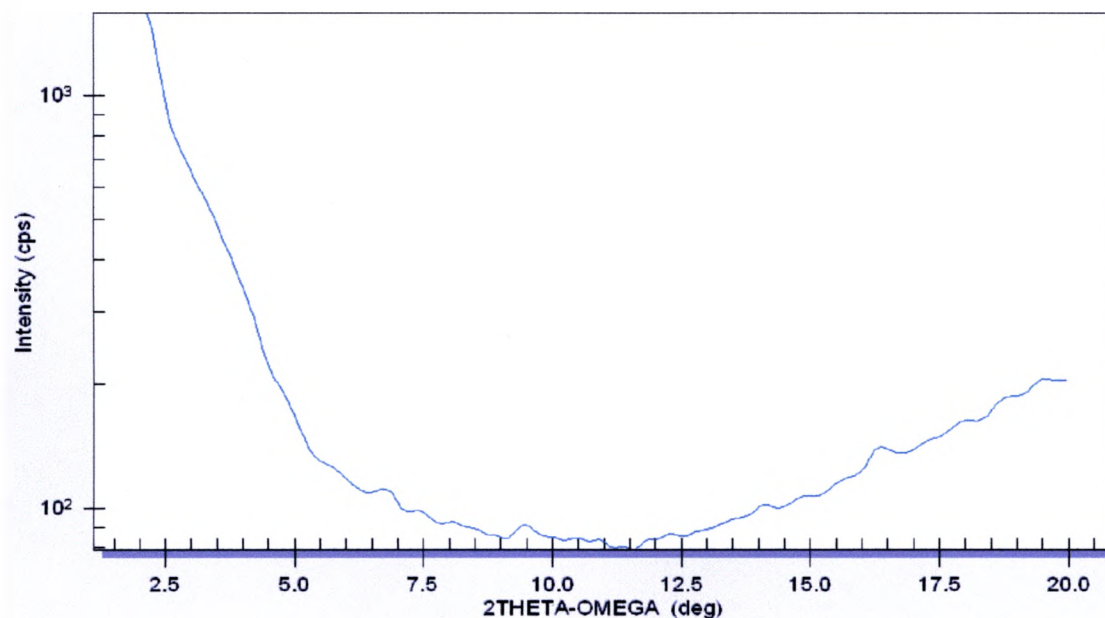


**Figure 33: Bede x-ray diffraction pattern for Pellethane.**

### 3.3.1 Quaternary Ammonium Surface Treated Clay-polymer Nanocomposite

Table 12 depicts the basal spacing and the intensity for the quaternary ammonium treated clays. The values were used to determine whether the clay is intercalated or exfoliated into the polymer matrix. The ladder series of quaternary ammonium salt showed an increase in d- spacing compared to the untreated clay. The increased gallery for the 2HT clay is due to the quaternary ammonium ions replacing the sodium ions on the surface of each clay layer. The quaternary ammonium ions push the plates apart. For this series, the 95 m.eq. exchange of 2HT on the surface of the clay increased the d- spacing to 39.24 Å (figure 34). Once the exchange capacity was increased above 95 m.eq. the d- spacing began to plateau. If the exchange capacity is underestimated, there will not be enough quaternary ammonium ions to exchange with all the sodium ions on the

clay surface and therefore the plates do not separate to an optimum value. If too much quaternary ammonium ion is added, the excess quaternary ammonium will wash out of clay and tends to plasticize the polymer.

| <i>Clay Treatments</i>                      | <i>Basal Spacing (d-spacing)<br/>(Å)</i> | <i>Intensity (cps)</i> |
|---|--|------------------------|
| <b>Quaternary Ammonium Salt 2HT (m.eq.)</b> |  |                        |
| 90  | 37.68                                    | 11800                  |
| 95  | 39.24                                    | 2020                   |
| 100   | 35.97                                    | 7000                   |
| 105   | 37.55                                    | 5890                   |
| 110   | 36.02                                    | 7500                   |

**Table 12: Quaternary ammonium salt 2HT nanocomposite first order x-ray diffraction peak (Å).**

There are also multiple peaks in each diffraction pattern, as shown in figure 34. The second and third peaks are simply second and third order peaks from the first diffraction. The multiple peaks indicates how well intercalated or exfoliated a system is. If there are no peaks, the system is completely exfoliated. If the first order peak is very weak, the system is intercalated with some exfoliation. If there are multiple peaks the system is intercalated, but not exfoliated. The more well ordered the system is, the more intercalated the system.

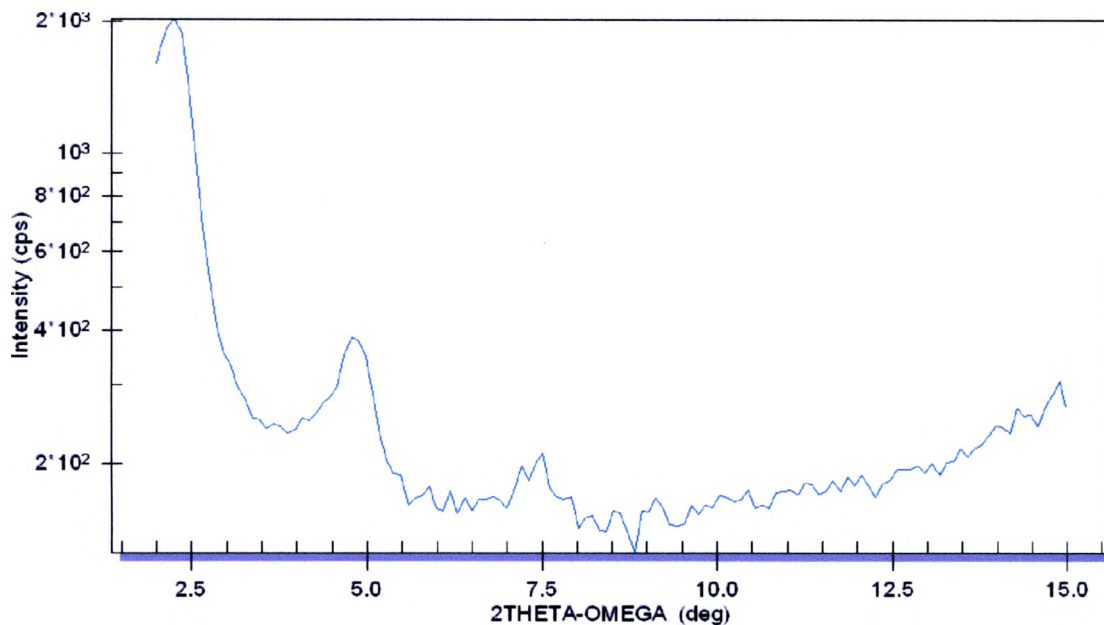


**Figure 34: Bede x-ray diffraction of 95/5 Pellethane and 95 m.eq. 2HT.**

### **3.3.2 Polymer and 2HT Surface Treated Clay-polymer Nanocomposite**

Both the PVP and the PPG were examined by XRD to determine which of the two sorption polymers promoted the most exfoliation. PVP and PPG, both in 2, 4, and 6 % by weight of the clay, exhibit an increase in the d-spacing compared to montmorillonite clay, but exhibit a decrease in the d-spacing compared to the 2HT organoclay. All of the treatments thus far demonstrated intercalation of the organoclay in the polymer matrix, but little exfoliation occurred. PPG was identified as the most compatible in the series because it had the lowest intensity overall, which demonstrates a higher extent of exfoliation.

| <i>Clay Treatments</i>                | <i>Basal Spacing (d-spacing)<br/>(Å)</i> | <i>Intensity (cps)</i> |
|---------------------------------------|--|------------------------|
| <b>PVP (%) 90 m.eq.2HT (200 mesh)</b> |  |                        |
| 2% PVP                                | 36.44                                    | 4150                   |
| 4% PVP                                | 35.63                                    | 7200                   |
| 6% PVP                                | 34.33                                    | 2840                   |

**Table 13: Polyvinyl pyrrolidone nanocomposite first order x-ray diffraction peak.**

| <i>Clay Treatments</i>     | <i>Basal Spacing (d-spacing)<br/>(Å)</i> | <i>Intensity (cps)</i> |
|----------------------------|--|------------------------|
| <b>PPG (%) 100m.eq.2HT</b> |  |                        |
| 2% PPG (325 mesh)          | 35.01                                    | 1060                   |
| 4% PPG (325 mesh)          | 36.40                                    | 3220                   |
| 6% PPG (325 mesh)          | 36.35                                    | 2150                   |

**Table 14: Polypropylene glycol nanocomposite first order x-ray diffraction peak.**

### 3.3.3 Edge, PPG, and 2HT Treated Clay-polymer Nanocomposite

The clay-polymer nanocomposites with all three treatments were also tested using XRD to determine the most exfoliated system with respect to the silanes. The edge treatments on the clay increased the gallery compared to the untreated sodium clay. Octadecyltrimethoxy silane, PPG, and 2HT organoclay at 325 mesh showed the greatest increase in d-spacing as well as no first order peak (figure 35). The absence of the first order peak was most likely due to the fact that the first order peak was buried in the main beam path. The d-spacing was calculated by using the second order peak and Bragg's law. The missing first order peak indicates a slightly exfoliated system, with some intercalation. The intensity of the first order peak is not available, but the intensity of the second order peak is 220 counts per second (cps) which signifies a slight intercalation in the nanocomposite matrix. The next lowest intensity for a second order peak is the phenyltrimethoxy silane treatment at 470 cps (325 mesh) and 560 cps (200 mesh). Even

though the intensity is low, 3-aminotrimethoxy silane was chosen as the next best nanocomposite with respect to the silane because the 325 mesh had a fourth order peak, signifies a highly intercalated system (figure 36). The diffraction pattern is plotted as d-spacing, in angstroms, versus the natural log (ln) intensity (cps) to display the 4 peaks.

| <i>Clay Treatments</i>                   | <i>Basal Spacing (d-spacing)<br/>(A)</i> | <i>Intensity (cps)</i> |
|--|--|------------------------|
| <b>Edge Treatment 2%PPG 100m.eq. 2HT</b> |  |                        |
| 3-Aminotrimethoxy Silane (200mesh)       | 35.35                                    | 5000                   |
| 3-Aminotrimethoxy Silane (325mesh)       | 35.31                                    | 8000                   |
| Dodecyltrimethoxy Silane (200mesh)       | 36.09                                    | 8500                   |
| Dodecyltrimethoxy Silane (325mesh)       | 33.16                                    | 19000                  |
| Octadecyltrimethoxy Silane (200mesh)     | 36.82                                    | 5000                   |
| Octadecyltrimethoxy Silane (325mesh)     | 37.56                                    | N/A                    |
| Phenyltrimethoxy Silane (200mesh)        | 35.35                                    | 600                    |
| Phenyltrimethoxy Silane (325mesh)        | 35.35                                    | 450                    |
| Vinyltrimethoxy Silane (200mesh)         | 35.24                                    | N/A                    |
| Vinyltrimethoxy Silane (325mesh)         | 35.35                                    | 7400                   |

**Table 15: Edge treatment nanocomposite first order x-ray diffraction peak.**

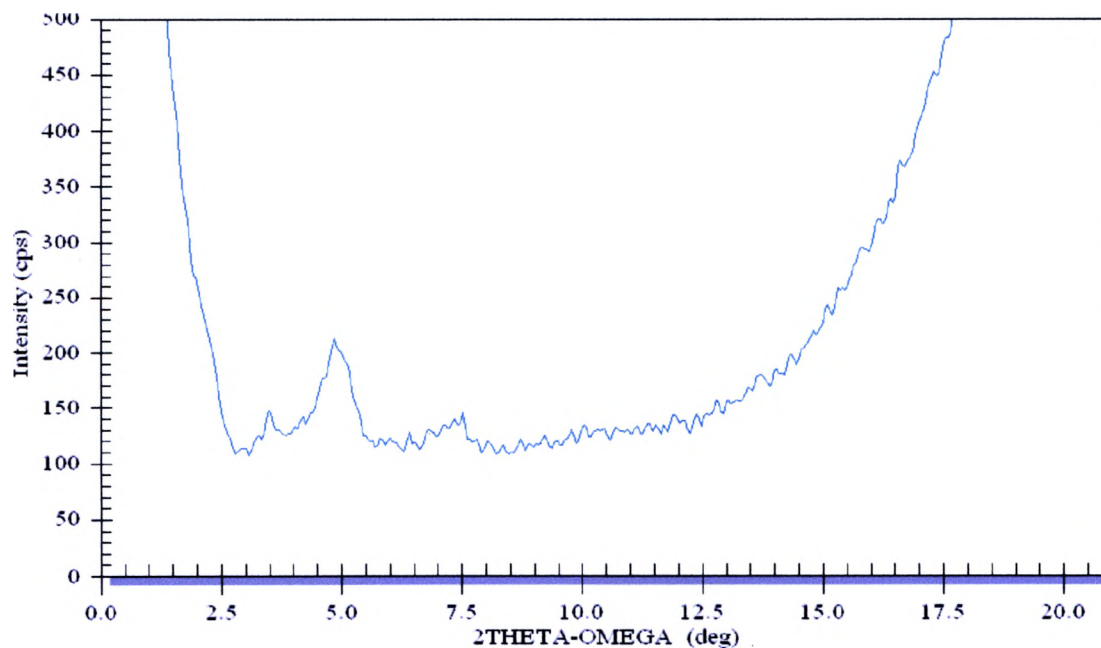


**Figure 35: Octadecyltrimethoxy Silane (325 mesh) x-ray diffraction pattern.**

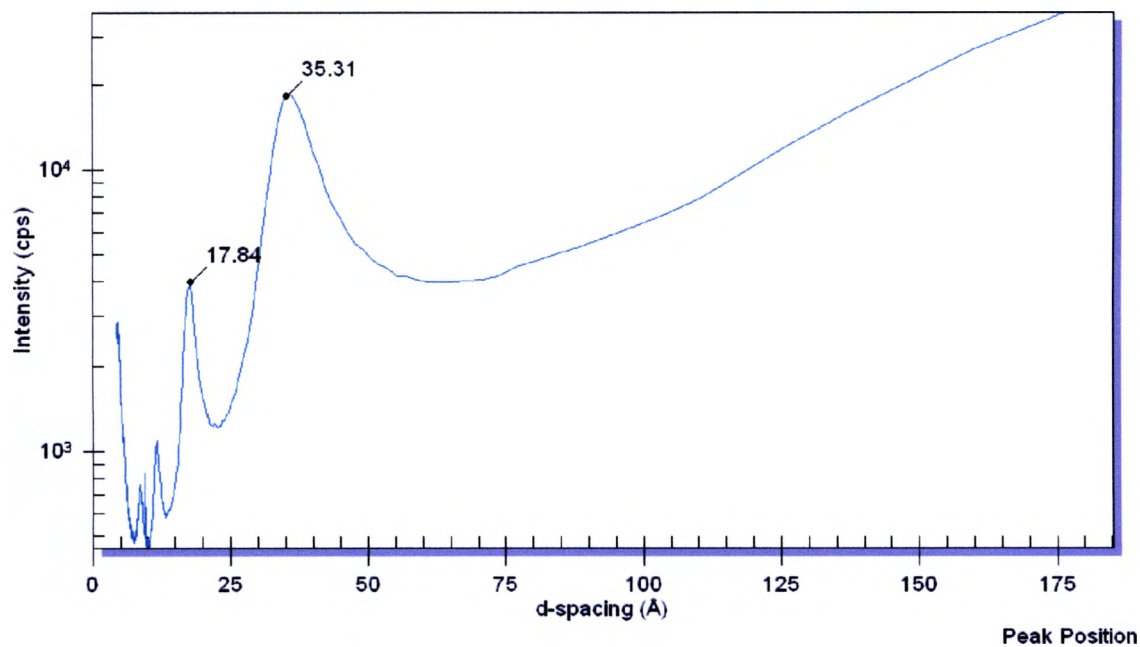


**Figure 36: 3-Aminotrimethoxy Silane (325 mesh) x-ray diffraction pattern.**

### **3.3.4 Edge and 2HT Treated Clay-Polymer Nanocomposite**

The d-spacing and the intensity of the edge and quaternary ammonium treated clays are described in Table 16. The organoclay without the PPG treatment exhibits a drastic increase in intensity, which indicates that the PPG is actually increasing the intercalation in the system. Without the PPG surface treatment, the intensity increased 230 % for the 3-aminotrimethoxy silane (325 mesh) and 840% for the octadecyltrimethoxy silane (200 mesh).

| <i>Clay Treatments</i>                  | <i>Basal Spacing (d-spacing)<br/>(Å)</i> | <i>Intensity (cps)</i> |
|---|--|------------------------|
| <b>100 m.eq. 2HT and Edge Treatment</b> |  |                        |
| 3-Aminotrimethoxy Silane (200mesh)      | N/A                                      | N/A                    |
| 3-Aminotrimethoxy Silane (325mesh)      | 35.31                                    | 18500                  |
| Octadecyltrimethoxy Silane (200mesh)    | 36.03                                    | 42000                  |
| Octadecyltrimethoxy Silane (325mesh)    | 37.56                                    | 4900                   |

**Table 16: Edge and 2HT treatment nanocomposite first order x-ray diffraction peak.**

### 3.3.5 Washed Edge, PPG, and 2HT Treated Clay-polymer Nanocomposite

As with the DMTA and tensile testing, the washed series of nanocomposites were tested by XRD and the results are tabulated below (table 17). The washed organoclay exhibit no improvement in exfoliation as shown by x-ray diffraction. The intensity increased for both the 3-aminotrimethoxy silane and the octadecyltrimethoxy silane which indicates a more intercalated system without washing the organoclay. Also, the d-spacing for both are within the deviation of the nanocomposite that was not washed, which means the gallery has not increased.

| <i>Clay Treatments</i>                        | <i>Basal Spacing (d-spacing)<br/>(Å)</i> | <i>Intensity (cps)</i> |
|---|--|------------------------|
| <b>Washed 100 m.eq. 2HT, 2% PPG, and E.T.</b> |  |                        |
| 3-Aminotrimethoxy Silane                      | 36.069                                   | 12500                  |
| Octadecyltrimethoxy Silane                    | 36.054                                   | 18000                  |

**Table 17: Washed edge, PPG, and 2HT treatment nanocomposite first order x-ray diffraction peak.**

### 3.3.6 X-ray Diffraction Patterns For 100 m.eq 2HT Nanocomposite, 100 m.eq. 2HT & 4% PPG Nanocomposite and 100 m.eq. 2HT, 4% PPG, & 2% 3-Aminotrimethoxy silane Nanocomposite

The x-ray diffraction patterns for 100 m.eq 2HT nanocomposite, 100 m.eq. 2HT & 4% PPG nanocomposite and 100 m.eq. 2HT, 4% PPG, & 2% 3-aminotrimethoxy silane

nanocomposite have 2 different types of peaks. The first series of peaks are diffracted x-rays off the Basal spacing (0, 0, 1). The second series of peaks correspond to the A-B plane (h, k, 0) near  $25^\circ 2\theta$ . The ratio between the A-B plane and the Basal spacing normalize the counts per second because the A-B plain is consistent throughout montmorillonite. The counts per second indicate the extent of exfoliated in the system. If the counts are low, the system is more exfoliated than if the counts are high. The lower the ratio, the more exfoliation in the system.

The 100 m.eq. 2HT quaternary ammonium clay-polymer nanocomposite indicated that the system was very well intercalated (figure 37). The first peak on the diffraction pattern is the second order peak for the Basal spacing. The first order peak is near  $2.5^\circ 2\theta$ , but the scan ran from  $3-80^\circ 2\theta$ , so the first peak was not reported. The A-B plane peak diffracted at  $25^\circ 2\theta$  as expected. To normalize the Basal spacing the ratio between the counts per second for the second order peak and the A-B plane was calculated (table 18). The 100 m.eq. 2HT & 4% PPG clay-polymer nanocomposite and the 100 m.eq. 2HT, 4% PPG, & 2% 3-aminotrimethoxy silane clay-polymer nanocomposite were also normalized to the A-B plane (figure 38 and 39). The ratio indicates that the exfoliation is increasing and the intercalation decreasing with the addition of each clay treatment. The surface only treated nanocomposite had a ratio of 1.22 while the surface and polymer surface treated nanocomposite had a ratio of 1.08. The best ratio is the nanocomposite with all three treatments having a ratio of only 0.31.

| Nanocomposite   | Ratio |
|---|-------|
| 100 m.eq. 2HT   | 1.22  |
| 100 m eq. 2HT & 4% PPG                                | 1.08  |
| 100 m.eq. 2HT, 4 % PPG, & 2% 3-aminotrimethoxy silane | 0.31  |

**Table 18: Height ratio of the A-B plane and the Basal spacing.**

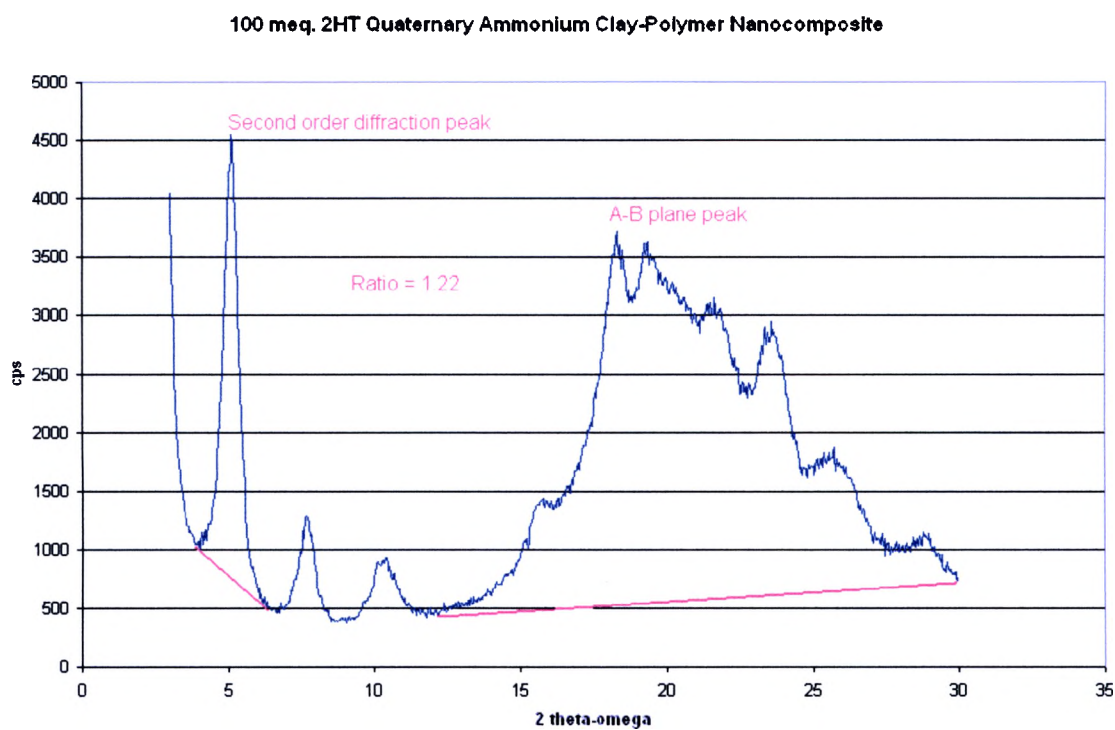


**Figure 37: X-ray diffraction pattern for the quaternary ammonium surface treated nanocomposite.**

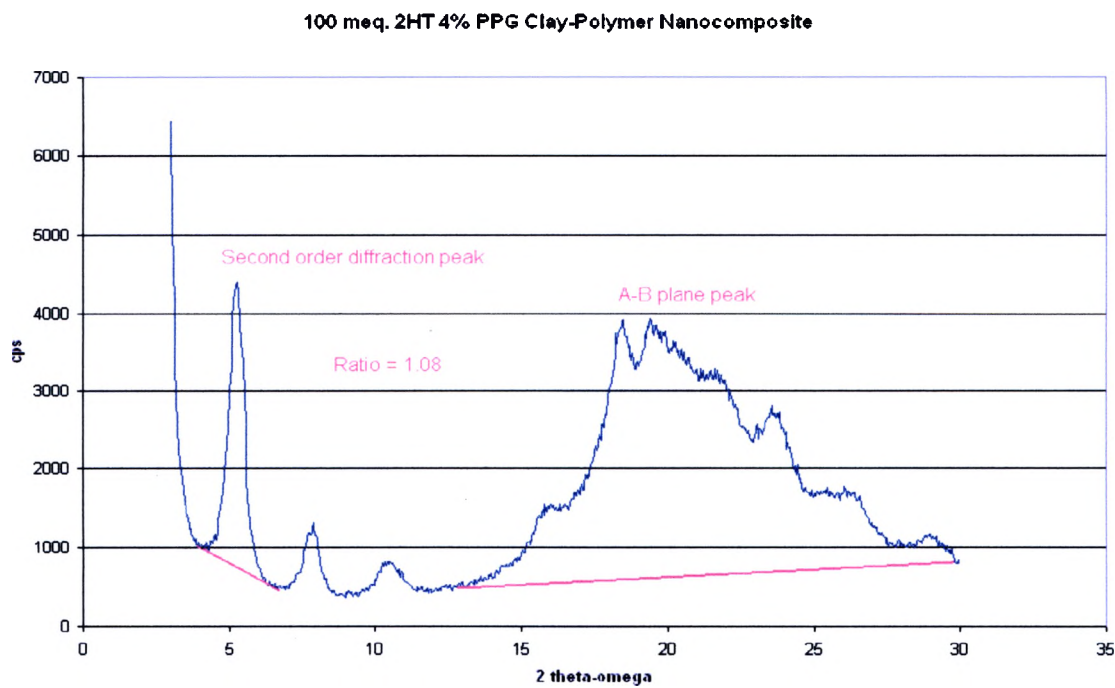


**Figure 38: The x-ray diffraction pattern for the quaternary ammonium and polymer surface treated nanocomposite.**

## 100 m.eq. 2HT 4% PPG 2% 3-AminoSilane Clay-Polymer Nanocomposite

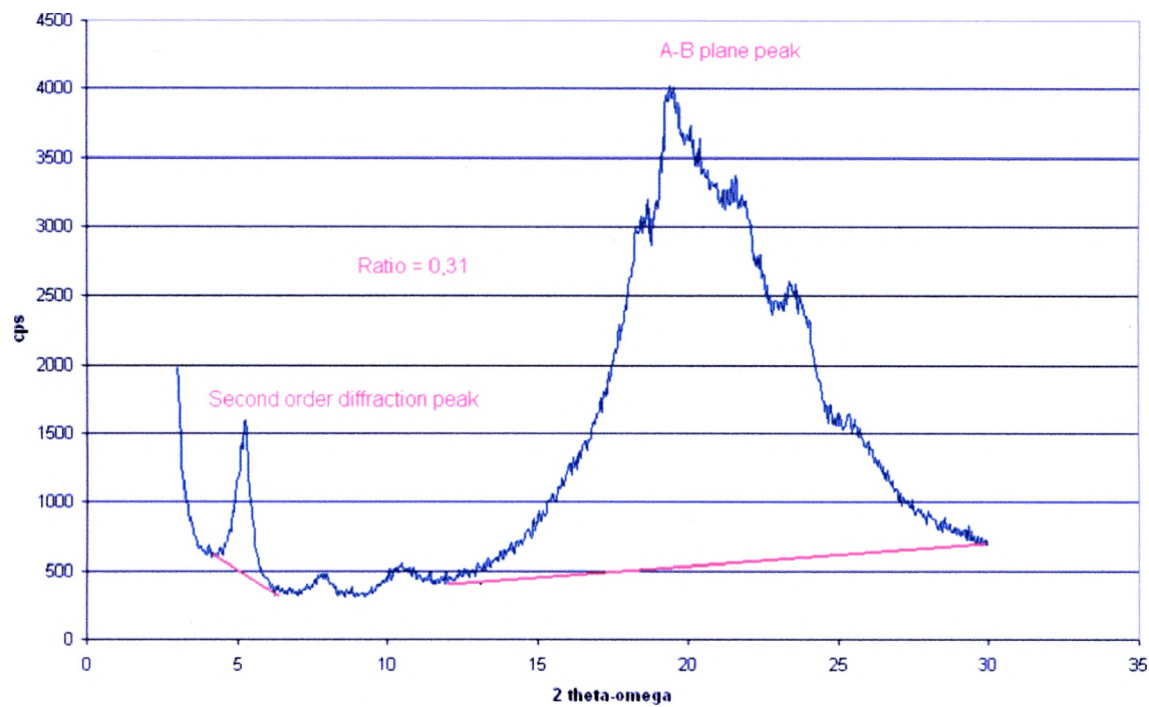


**Figure 5: The x-ray diffraction pattern for the quaternary ammonium, polymer, and edge treated nanocomposite.**

## 4.0 CONCLUSION

### 4.1 Surface Treated Clay-polyurethane Nanocomposites

After reviewing all of the data on the quaternary ammonium surface treatment, the nanocomposites showed improved properties when compare to the pristine polymer. The gallery size was doubled compared to untreated montmorillonite. The 2HT quaternary ammonium series had a d-spacing of 35.97 to 39.24 angstroms, while montmorillonite had a d-spacing of 12.5 angstroms. The increased gallery allowed for the polymer to enter in-between two clay platelets and assist the exfoliation. The 2HT quaternary ammonium treatment did not cause the complete exfoliation of the nanocomposite, but it increased the physical properties. The storage modulus increased by at least 100% for the ladder series of quaternary ammonium clay-polymer nanocomposite. The pristine polymer had a modulus of 15.98 ( $\pm 2.87$ ) MPa, while the 100 m.eq. 2HT clay-polymer nanocomposite displayed a modulus of 42.50 MPa which correspond to a 165% increase. The composite made with PPG and edge treatment yielded a macroscale composite with 35.99 MPa modulus. The modulus observed for quaternary ammonium treatment alone compared to theoretical calculations of 60 MPa would indicate that the clay was mostly intercalated with some exfoliation.

The Young's modulus also increased drastically compared to the pristine polymer. The 100 m.eq. 2HT clay-polymer nanocomposite increased Young's modulus 95% compared to the pristine polymer. The 100 m.eq. 2HT clay-polymer nanocomposite did

fail under 117.2 (N), while the pristine polymer was let go by the grips. No evidence can be drawn with regards to the peak load of the pristine polymer. Even if full exfoliation was not achieved, the quaternary ammonium surface treatment increased the physical properties because the quaternary ammonium allowed more polymer to go into the gallery. Once the polymer is in the clay gallery, the clay act as reinforcement, analogous to steel rebars in concrete.

#### **4.2 Surface and Sorption Surface Treated Clay-polyurethane Nanocomposite**

Following the assessment of the data involving the 2HT and surface sorption treatment, the findings were that the PPG helped the physical properties of the nanocomposites while increasing exfoliation slightly. The basal spacing was increased compared to the pristine polymer, but it was not increased compared to just the 2HT treated clay-polymer nanocomposite. The ratio between the A-B plane and the second order peak however, did indicate that the exfoliation increased slightly from the nanocomposite with only the quaternary ammonium surface treatment.

The storage modulus increased by 15% when 4% PPG was on the surface compared to the 100 m.eq. 2HT clay-polymer nanocomposite, which indicates that there is exfoliation and intercalation in the clay-polymer nanocomposite. The PPG also showed definite signs of an optimization level, while the PVP actually hindered the exfoliation.

The Young's modulus also increased compared to the pristine polymer, but compared to the other nanocomposites, the tensile test was not sensitive to each treatment. The surface and PPG treated nanocomposite also failed under stress. Therefore, the pristine polymer can handle more stress as compared the treated clay-polymer nanocomposite.

The reason the nanocomposites were failing under low stress was because of the processing procedure. If the processing procedure was optimized, the nanocomposite should be able to withstand a higher stress before failing.

#### **4.3 Surface, Sorption Surface, and Edge Treated Clay-polyurethane Nanocomposite**

The silane edge treatment helped the exfoliation. The X-ray diffraction pattern indicated that the nanocomposite with all three treatments had the lowest A-B plane to second order peak ratio and, therefore the nanocomposite with all three treatments was the most exfoliated system. For the octadecyltrimethoxy silane edge treatment, the diffraction pattern even showed that the system was exfoliated with some intercalation. The d-spacing did not increase as compared to the clay with the surface treatment or the surface/sorption treated clay. Neither the DMTA nor the tensile test showed any dramatic improvements in the physical properties as compared to the nanocomposite with surface and sorption treatments. However, the DMTA did indicate that these clay-polymer nanocomposites have a storage modulus in the range, which correlates to a combination of intercalated and exfoliated systems as compared to the theoretical calculations. The results indicate that the edge treatment does help the exfoliation process, but has limited effect on the physical properties. The reason it helps exfoliation is that the edges are no longer a barrier for the polymer to enter into the gallery. Even though the edge helps exfoliation, the physical properties did not show an increase as compared to the nanocomposites without the edge treatment because the tensile testing equipment was not sensitive enough to indicate whether each treatment helped the physical properties.

#### **4.4 Washed, Surface, Sorption, or Edge Treated Clay-polyurethane Nanocomposite**

The most remarkable result is the nanocomposite with the PPG and edge treated clay. This system showed dramatically different peak loads when compare to the other nanocomposites. The PPG and edge treated nanocomposites did not fail; they showed tensile load properties equal to that of the pristine polymer. They also displayed an increase in Young's modulus. There was however a decrease in clarity of the nanocomposite.

The washed clay and the surface and edge treated clays did not show any improvement as compared to the nanocomposites with one or more treatments. The one exception was the washed 3-aminotrimethoxy silane treated clay-polymer nanocomposite. The washed clay-polymer nanocomposites had relatively the same d-spacing, storage modulus, and Young's modulus.

#### **4.5 Final Conclusion**

The three treatments in conjunction with each other did provide evidence that they each contribute to the exfoliation process and to the physical properties of the systems themselves. However, there were several processes that could be improved upon to create a more exfoliated nanocomposite and increase the peak load. The first procedural process would be to twin screw extrude the nanocomposite. The extrusion would allow a higher shear, which in turn assists the exfoliation process. When the shear is increased, the clay platelets are pulled apart so that more polymer can go in-between the platelets and increase the gallery spacing.

The second procedural process which would help is to injection mold the nanocomposites into tensile bars. Injection molding would increase the peak load capability of each nanocomposite containing the 2HT quaternary ammonium surface treatment. There would be less of a chance of the lamination effect of taking place. Injection molding creates a more unified nanocomposite matrix. If these two procedures were employed, the nanocomposites would come closer to being exfoliated instead of intercalated.

## REFERENCES

- 1) Brill, B. Nanoclays – counting on consistency. Southern Clay Products Inc. **1-7** (2003).
- 2) Stackhouse, S.; Conveyeney, P.V.; Sandré, E. Plane-wave density function theoretic study of formation of clay-polymer nanocomposite material by self-catalyzed in situ intercalative polymerization. *J. Am. Chem. Soc.* **123**, **11764-11774** (2003).
- 3) Kornmann, X. Synthesis and characterization of thermoset-clay nanocomposites. *Luleå Univ. of Tech. Division of Polymer Engineering.* **1-29**(1999).
- 4) LeBaron, P.C.; Wang, Z.; Pinnavaia, T.J. Polymer-layered silicate nanocomposites: overview. *Applied Clay Science.* Vol. **15**, **11-29** (1999)
- 5) Wang, Z.; Pinnavaia, T.J. Nanolayer reinforcement of elastomeric polyurethane. *Chem. Mater.* Vol. **10**, **3769-3771** (1998).
- 6) Usuki, A.; Kojima, Y.; Kawasumi, M.; Okada, A.; Fukushima, Y.; Kurauchi, T., Kamigaito, O.; *J Mater Res* 1993;8(5):**1179-84**.
- 7) Usuki, A.; Kojima, Y.; Kawasumi, M.; Okada, A.; Fukushima, Y.; Kurauchi, T.; Kamigaito, O.; Nylon-6 clay hybrid, *Mater.Res.Soc.Proc* ,171,**45-50** (1990)
- 8) Kawasumi, M.; Kohzaki, M.; Kojima, Y.; Okada, A.; Kamigaito, O.; United States Patent Number 4810734; 1989 (assigned to Toyota Motor Co., Japan)
- 9) Kojima, Y.; Usuki, A.; Kawasumi, M.; Okada, A.; Kurauchi, T.; Kamigaito, O., *J. Appl. Polym. Sci.* Vol. **49**, **1259-64** (1993)

- 10) Kim, B.K.; Seo, J.W.; Jeong H.M. Morphology and properties of waterborne polyurethane/clay nanocomposites. *European Polymer J.* Vol.39, **85-91** (2003).
- 11) Lopez-Manchado, M.A.; Arroyo, M., Herrero, B.; Biagiotti, J. Vulcanization kinetics of natural rubber-organoclay Nanocomposite. *J. of Applied Polymer Science*, Vol. 89, **1-15** (2003).
- 12) Chin, J.C.; Martin, D.J. Synthesis and characterization of polyurethane/ clay nanocomposite: melt compounding. *The Univ. Queensland. Dept. Of Engineering.* **1-26** (2002).
- 13) Pinnavia, T J.; Beall, G.W. Polymer-clay nanocomposites. *Wiley Series in Polymer Science*, **97-109, 197-205** (2000).
- 14) Stevens, M.P. Polymer chemistry an introduction. *Oxford Univ. Press.***110-112**, (1999)
- 15) Kim, J.; Jung, W.; Park, K.; Suh, K. Synthesis of Na<sup>+</sup> montmorillonite/ amphiphilic polyurethane nanocomposite via bulk and coalescence emulsion polymerization *J. Applied Polymer Science*, Vol. 89, **3130-3136** (2003)
- 16) [www.nanocor.com/glos\\_pop.htm](http://www.nanocor.com/glos_pop.htm)
- 17) Mishra, J.K.; Kim, I.; Ha, C. New millable polyurethane/ organoclay nanocomposite, preparation, characterization and properties. *Macromol. Rapid Commun.* Vol. 24, **671-675** (2003).
- 18) Fornes, T.D.; Yoon, P.J.; Keskkula, H.; Paul, D.R. Effect of organoclay structure on nylon 6 nanocomposite morphology and properties *Polymer.* Vol. 43, **5915-5933** (2002)

- 19) Gilman, J.W. Flammability and thermal stability studies of polymer layered-silicate (clay) nanocomposites. *Applied Clay Science* Vol. 15, Issue 1-2, **31-49** (1999)
- 20) Allcock, H.R.; Lampe, F W. Contemporary polymer chemistry. Prentice Hall, New Jersey. **524-535**.
- 21) [http://www.rlHUDSON.com/tech\\_thermo.html](http://www.rlHUDSON.com/tech_thermo.html)
- 22) [www.psrc.usm.edu/macrog/urethane.htm](http://www.psrc.usm.edu/macrog/urethane.htm)
- 23) Brody, A L “Nano, nano” food processing technology. *Food Technology*. Vol. 57, No. 12, **52-54** (2003).
- 24) Fornes, T.D., Paul, D.R., *Macromolecules*, Vol. 37, **7698-7709** (2004).

## VITA

Elizabeth Ann Peterson was born on May 24, 1979, in a small town of Three Rivers, Michigan, the daughter of Jae Boon Kim and George William Peterson. She graduated from Cypress Falls High School, Houston, Texas, in 1997 and continued her education at Texas State University-San Marcos, where she earned a Bachelor of Science with a double major in Chemistry and Environmental Studies in May 2003. In August 2003 she furthered her education by entering the Texas State University-San Marcos Graduate Program, San Marcos, Texas, for a Master of Science Degree in Chemistry.

Permanent Address:           1269 Hilltop Dr.  
  San Marcos, Texas 78666

This thesis was typed by Elizabeth Ann Peterson

